Applied Geochemistry 152 (2023) 105630

Contents lists available at ScienceDirect

Applied Geochemistry

journal homepage: www.elsevier.com/locate/apgeochem

Geochemical modeling of CO_2 sequestration in ultramafic mine wastes from Australia, Canada, and South Africa: Implications for carbon accounting and monitoring

Carlos Paulo [a,*], Ian M. Power [a], Nina Zeyen [b,1], Baolin Wang [b], Siobhan A. Wilson [b]

[a] Trent School of the Environment, Trent University, Peterborough, Ontario, K9L 0G2, Canada
[b] Department of Earth and Atmospheric Sciences, University of Alberta, Edmonton, Alberta, T6G 2E3, Canada

ARTICLE INFO

Editorial Handling by: Dr. Robert Seal

ABSTRACT

Passive carbonation in ultramafic mine wastes results from the spontaneous reaction of gangue minerals with carbon dioxide (CO_2) to form stable carbonate minerals that store CO_2. Mines can benefit from unintentional CO_2 sequestration to offset greenhouse gas (GHG) emissions. Quantitative X-ray diffraction (QXRD) analysis of numerous samples of mine wastes has typically been used to quantify passive carbonation rates. This analysis yields valuable information about carbon sinks; however, extensive mineralogical assessments are technically demanding and cost-prohibitive for routine carbon accounting. Alternatively, we explored using inverse geochemical modeling to estimate passive carbonation rates and monitor CO_2 sequestration in active mines. Water chemistry data, tailings mineralogy, and operational information routinely collected by mines were used as inputs for models. The predictive capabilities of the models were tested for Mount Keith nickel mine (Australia), Diavik diamond mine (Canada) – for which rates were previously determined using QXRD. A new site — Venetia diamond mine (South Africa) — was used to illustrate the potential of geochemical modeling for carbon accounting and as a long-term monitoring tool for CO_2 sequestration. Mount Keith models predicted passive carbonation rates (3900 g $CO_2/m^2/yr$) consistent with previous QXRD assessments (2400 g $CO_2/m^2/yr$; 172 samples) using only two water samples. CO_2 removal rates for Diavik were found to be impacted by seasonality and to range between ~375 and 510 g $CO_2/m^2/yr$, showing similarities with previous QXRD rates estimates (313–350 g $CO_2/m^2/yr$). With the long-term water chemistry records (2009–2018) available for Venetia mine, we predicted calcite as the main CO_2 sink and that ~14,875 t CO_2 were stored in the kimberlite residues impoundments (3.5 km^2) over 9 years at a rate of ~470 g $CO_2/m^2/yr$. Moreover, long-term monitoring shows a decline in CO_2 removal rates at Venetia, possibly due to changes in kimberlite reactivity and current mine waste disposal practices. Overall, inverse modeling proved that it can be a viable alternative or complement to QXRD techniques for carbon accounting in active mines, substantially reducing the need for mine waste sampling and permitting long-term monitoring. Moreover, the model shows how passive carbonation rates change dynamically with the mine production and waste management practices. Simultaneously, the model provides insights into potential mineral reactions operating in tailings and that regulate carbon sequestration mechanisms. For that reason, this accounting technique has an enormous potential to assist in decision-making for implementing enhanced CO_2 sequestration strategies (e.g., enhanced rock weathering) and to support carbon sequestration monitoring, validation, and reporting in active mines.

1. Introduction

Broad implementation of negative emission technologies (NETs) for carbon dioxide removal (CDR) is necessary to reach carbon neutrality by 2050 and net negative emissions of carbon dioxide (CO_2) afterward (Haszeldine et al., 2018; Minx et al., 2018; National Academies of Sciences, 2019). CO_2 mineralization and enhanced rock weathering (ERW) are two NETs that involve weathering of mineral powders and industrial

* Corresponding author.
E-mail addresses: cfernandesesilvapaul@trentu.ca, carlos.fernandesesilvapaulo@mail.utoronto.ca (C. Paulo).
[1] Now at Department of Earth Sciences, University of Geneva, 1205 Geneva, Switzerland.

https://doi.org/10.1016/j.apgeochem.2023.105630
Received 7 November 2022; Received in revised form 18 February 2023; Accepted 15 March 2023
Available online 21 March 2023
0883-2927/

wastes to remove CO_2 from the atmosphere. Natural mineral weathering has regulated atmospheric CO_2 concentrations over geologic time and is estimated to consume ~1 Gt CO_2/yr (Hartmann et al., 2009; Moosdorf et al., 2014; Zhang et al., 2021). The goal of mineral weathering-based technologies is to accelerate natural weathering and store CO_2 as either a soluble phase (HCO_3^-), i.e., solubility trapping of CO_2, or a solid carbonate mineral (e.g., $CaCO_3$), i.e., mineral trapping of CO_2 (IPCC et al., 2019; Sandalow et al., 2021).

Several similarities exist between CO_2 mineralization in mine waste impoundments and ERW. Existing mines with (ultra)mafic tailings are, in essence, large land areas containing 10–100s of megatonnes of mineral powders (commonly <1 mm). Ultramafic and mafic mine wastes are composed of magnesium- and calcium-bearing minerals, including olivine (e.g., forsterite: Mg_2SiO_4), diopside ($CaMgSi_2O_6$), serpentine (e.g., lizardite: $Mg_3Si_2O_5(OH)_4$), and brucite ($Mg(OH)_2$) that are targeted for CO_2 mineralization and ERW (cf. Assima et al., 2014; Bodénan et al., 2014; Daval et al., 2009; Huijgen et al., 2006; Power et al., 2014; Thom et al., 2013; Wilson et al., 2011). In ERW dispersal areas and mine waste impoundments, rock powders/tailings are spread over large areas — albeit for different purposes — and left exposed to weather for extended periods (Amann et al., 2020; Moosdorf et al., 2014; Schuiling and Krijgsman, 2006). Mineral reactivity determines the ability of rock powders to remove CO_2 from the atmosphere, which at ambient conditions is primarily dominated by the cations that can be easily extracted from minerals (Lu et al., 2022b; Paulo et al., 2021; Stubbs et al., 2022). Mineral dissolution by carbonic acid (H_2CO_3) releases divalent cations (e.g., Mg^{2+} and Ca^{2+}), increases alkalinity, and if the mineral saturation state and kinetics are favorable, carbonate minerals can precipitate to store CO_2 (Power et al., 2013). Mineral trapping in ultramafic tailings frequently occurs as secondary magnesium carbonates, including hydromagnesite $Mg_5(CO_3)_4(OH)_2{\cdot}4H_2O$], dypingite [$Mg_5(CO_3)_4(OH)_2{\cdot}{\sim}5H_2O$], and nesquehonite ($MgCO_3{\cdot}3H_2O$) (Beaudoin et al., 2017; Lechat et al., 2016; Oskierski et al., 2021; Power et al., 2014; Turvey et al., 2017; Wilson et al., 2011). Mineral weathering by CO_2 is accelerated in tailings, and since the geochemical processes that lead to CO_2 sequestration are essentially the same, mines can be suitable sites for developing long-term monitoring, validation, and reporting tools for ERW.

Passive carbonation, i.e., unintentional carbonation, has been documented in ultramafic tailings (e.g., asbestos, diamond, and nickel mines) at both active and abandoned mines (cf. Assima et al., 2013a; Bea et al., 2012; Hamilton et al., 2021; Meyer et al., 2014; Power et al., 2013; Wilson et al., 2011; Wilson et al., 2014; Wilson et al., 2009). In the past, extensive mineralogical surveys using numerous mine waste samples have been used to estimate passive carbonation rates supported by the abundance of secondary carbonate minerals in tailings (Hamilton et al., 2021; Turvey et al., 2017, 2018; Wilson et al., 2009, 2011). Although these mineralogical assessments yield valuable information about cation sources and carbon sinks, they are technically demanding, require extensive sampling and specialized models for mineral identification and quantification, and have limited accuracy in quantifying low-abundance minerals (<2% wt.). Therefore, mineralogical assessments can be technically demanding and likely cost-prohibitive for routine monitoring of CO_2 sequestration, particularly for active mines. Moreover, these assessments do not provide insights into solubility trapping, the first sink for atmospheric carbon via chemical weathering in terrestrial and aqueous environments (Gaillardet et al., 1999; Hartmann et al., 2009), which has largely been overlooked as a carbon sink in mines.

Most ultramafic mine wastes are deposited as a slurry of finely pulverized rock and water in large impoundments (km^2–scale) that function as basins where waters are circulated to and from processing plants (Power et al., 2014; Stubbs et al., 2022). For that reason, mine waste impoundments are comparable to small catchment basins draining a specific rock type. Weathering of silicate and carbonate rocks in natural watersheds modifies the water chemistry baseline (Amann et al., 2020; Taylor et al., 2021), producing element fluxes between an initial and a final water composition that are quantifiable using mass-balance models. Similarly, mineral–water reactions occurring in the mineral processing circuit and within tailings impoundments strongly influence the composition of mine waters (e.g., porewaters in tailings) and carbon consumption rates in the mine waste impoundments.

Mines often sample and analyze numerous surface and ground waters to meet regulatory requirements. These monitoring programs result in detailed records of water chemistry throughout the life of a mine, which, when paired with relevant operational data, can be used in geochemical models to assess CO_2 sequestration. These models help determine the predominant chemical weathering processes, element mobility, and potential carbon sinks (Bricker et al., 2003; Frondini et al., 2019), as investigated by Rollo and Jamieson (2006) for the Ekati diamond mine (Canada).

Here, we demonstrate how mass-balance geochemical models (inverse modeling) can be a viable alternative or complement to mineralogical assessments to quantify CO_2 sequestration rates at the mine scale (km^2 and 10 s ML/yr). The predictive capabilities of the models were tested for the Mount Keith nickel mine (Australia) and Diavik diamond mine (Canada) and compared with previous passive carbonation rates obtained through extensive mineralogical assessments. In addition, modeling was applied to a new site — Venetia diamond mine (South Africa) — to estimate the passive carbonation rate and illustrate how a long-term monitoring program for carbon sequestration can be implemented in active mines using existing water quality data. With the growing implementation of national and international carbon markets and the pressure to reach carbon neutrality, ultramafic mine tailings will rapidly become a vital feedstock for CO_2 sequestration. Our study contributes to the development of geochemical modeling tools designed to assist decision-making in implementing CO_2 sequestration strategies and supporting carbon sequestration monitoring, validation, and reporting (MVR) programs for active mines.

2. Mine site descriptions

2.1. Mount Keith nickel mine

The Mount Keith nickel mine is a large open-pit operation in the world's largest dunite-hosted Archean nickel sulfide deposit (Brand and Butt, 2001). The mine has been operated by Nickel West, a division of BHP Group Ltd, since 2005. Mount Keith is located at 27°14′50″ S, 120°32′30″ E in the Northeastern Goldfields district of Western Australia (Fig. 1a). The region is affected by high temperatures (average annual temperature of 29 °C), and evaporation (up to 3600 mm/yr) largely exceeds the annual mean rainfall (260 mm).

The mine is hosted in serpentinized dunite enclosed by a larger peridotite-dunite komatiite with a lenticular structure designated the Mount Keith Ultramafic Complex (Brand and Butt, 2001). The deposit is dominated by sequences of weathered and serpentinized komatiites (Brand and Butt, 2001). The host rocks of this nickel deposit include volcanoclastic rocks, such as andesite and dacite, pyritic chert, tuffaceous volcanoclastic sedimentary rocks, graphitic shales, and basaltic rocks (Brand and Butt, 2001). The sulfide ore contains 0.52–0.58 wt% nickel, primarily hosted in iron–nickel sulfide minerals, such as pentlandite [$(Fe, Ni)_9S_8$], present in serpentinized olivine pseudomorphs (Brand and Butt, 2001; Wilson et al., 2014).

2.1.1. Mineral processing and mine waste management at Mount Keith

Mineral processing at Mount Keith is performed with froth flotation methods using saline groundwaters primarily obtained from regional borefields (Albions Downs, Caprock, South Lake Way) located within 50 km of the mine, as shown in Fig. 1a (MWES Consulting, 2017; Wilson et al., 2014). In 2006, the annual tailings production was estimated at ~11 Mt (Table 1), utilizing 9.5 × 106 m3 of processing water (Power et al., 2014; Wilson et al., 2014). The tailings are piped as slurries from

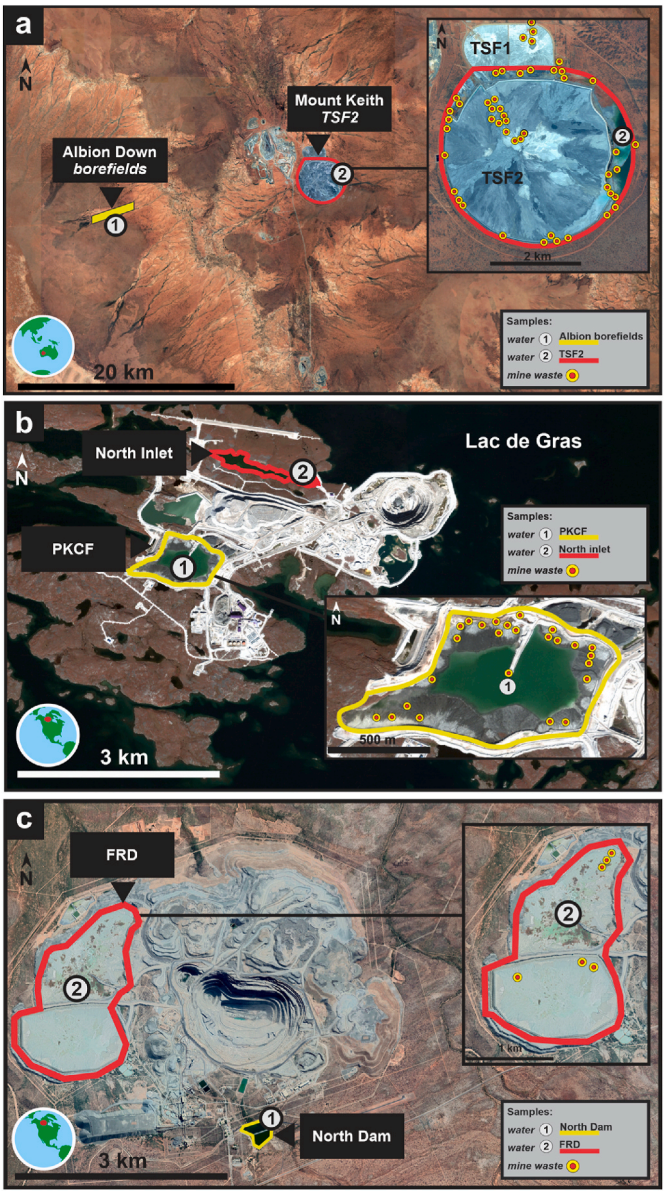

Fig. 1. Overview of the mine wastes impoundments, and the water and mine waste sampling locations in (a) Mount Keith nickel mine, Australia, (b) Diavik diamond mine, Canada, (c) Venetia diamond mine, South Africa. The solids sampling locations are indicated in the figures insets and correspond to the sites investigated by Wilson et al., (2014) (Mount Keith), Wilson et al., (2009) (Diavik), and Stubbs et al., (2022) (Venetia).

the processing plant to the Tailings Storage Facility 2 (TSF2; TSF1 was only operational from 1994 to 1997) and deposited as a slurry from spigots located on risers (Bea et al., 2012; Wilson et al., 2014). The seepage from the tailings impoundment is collected in a return dam (Fig. 1a) located on the east side of TSF2. These waters are frequently sampled as part of the environmental monitoring programs of the mine.

2.1.2. Mineralogy of the mine waste

Bea et al. (2012) and Wilson et al. (2014) reported detailed qualitative and quantitative mineralogy (summarized in Table 2) for Mount Keith tailings. The mineralogy was inferred from the analysis of hundreds of samples collected in April 2005 and September and October 2006. The sampling locations are indicated on Fig. 1a. Sampling was conducted along the TSF2 perimeter and service roads because large areas of the impoundment were saturated with process water and

Table 1
Summary of operational data used to calculate passive carbonation rates.

	Mount Keith	Diavik	Venetia
Location	Australia 27°14′50″S, 120°32′30″E	Canada 64°29′46″N, 110°16′24″W	South Africa 22° 25′ 59″ S, 29°18′50″ E
Geology	nickel sulphide deposit	kimberlite	kimberlite
Type of mine	Open-pit	Open-pit	Open-pit
Climate	arid	subarctic	semi-arid
Mean annual rainfall (mm)	260 mm	291 mm (50% snow)	200–400 mm
Mean annual evaporation (mm)	3200 to 3600 mm	275–315 mm	~2050 mm
Mean annual temperature (°C)	29 °C	−4.5 °C	22.4 °C
Operational data			
Water sources	Aquifer	Lac de Gras	Aquifer
Process water (m^3/yr)	~$9.5{\cdot}10^6$	~$2.3{\cdot}10^6$	~$3.0{\cdot}10^6$
Mine wastes production (Mt/yr)	11	2.5	4.74
Mine wastes reservoirs	TSF2	PKF	FRD
Area (km^2)	16.6	0.86	3.5
Water chemistry datasets	1998 (N = 2)	2004–2006 (N = 36)	2009–2018 (N = 70)
Inverse model			
Initial water	Pre-processing	PKF	North Dam
Final water	TSF2	North Inlet	FRD

Table 2
Mineralogy for mine wastes of Mount Keith, Diavik, and Venetia mines. Abundances were determined via Rietveld refinement with XRD data as reported in the literature.

Mine	Mineral	Ref.
Mount Keith	48.5−89.7 wt% serpentine; 1.1−11.3 wt% hydrotalcite; <6 wt% brucite; <5 wt% talc; 0.7−10.1 wt% magnetite and chromite; <5 wt% quartz; 0.4−13.6 wt% magnesite; 0.2−4.3 wt% dolomite; <1 wt% calcite; (<0.5 wt%) vermiculite or smectite; 2.5 wt% hydromagnesite	Wilson et al., (2014)
Diavik	40.0−76.2 wt% lizardite; 12.3−46.3 wt% high-Mg forsterite; 1.9−4.1 wt% calcite; 0.5−8.4 wt% vermiculite or smectite; <5 wt% plagioclase, <5 wt % diopside; <5 wt% quartz; 0−6.4 wt% pyrope-rich garnet; 1.6–3.5 wt% phlogopite; 0.50 wt% nesquehonite	Wilson et al., (2011)
Venetia	10.8−58.4 wt% lizardite; 6.2−39.9 wt% smectite; 2.4−10.3 wt% calcite; 1.1−22.0 wt% diopside; 0.8−6.0 wt% orthoclase; 6.3−21.1 wt% phlogopite; 0.6−10.7 wt% clinochlore; 0.9−6.2 wt% talc; 0.2−3.6 wt% quartz; 0.3−8.1 wt% tremolite; 2.4−8.7 wt% albite; 0.3−1.3 wt% magnetite; 0.1−1.3 hydroxylapatite	Zeyen et al., (2022)

inaccessible. Samples were randomly distributed and collected from cores and vertical sections on exposed surfaces and excavated trenches. Wilson et al. (2014) provide additional details regarding Mount Keith sampling.

Mount Keith mineralogy is highly favorable for CO_2 mineralization due to minor abundances (average 2.5 wt%) of brucite [$Mg(OH)_2$]. This mineral reacts rapidly with atmospheric CO_2 to form hydromagnesite at Mount Keith (Wilson et al., 2014). Serpentine minerals (48.5−89.7 wt% − antigorite, lizardite, and minor chrysotile [$Mg_3Si_2O_5(OH)_4$] are much less reactive yet are more abundant than brucite in Mount Keith tailings (Table 2). Hydrotalcite-group minerals (1.1−11.3 wt% — e.g., iowaite [$Mg_6Fe_2(OH)_{16}Cl_2{\cdot}4H_2O$]; woodallite [$Mg_6Cr_2(OH)_{16}Cl_2{\cdot}4H_2O$]; pyroaurite [$Mg_6Fe_2(OH)_{16}CO_3{\cdot}4H_2O$)]; and stichtite [$Mg_6Cr_2(CO_3$)

$(OH)_{16}{\cdot}4H_2O$] rapidly take up carbonate ions in exchange for interlayer chloride or sulfate ions; however, carbonation of these minerals is relatively inefficient as only one CO_2 molecule can be stored for every six magnesium atoms (Table 2). Secondary halide and sulfate minerals have also been reported in Mount Keith tailings (Wilson et al., 2014). These minerals form due to the high evaporation promoted by the regional arid climate conditions, which affects the water balance of the mine waste impoundments.

2.2. Diavik diamond mine

The Diavik diamond mine (64°29′46″N, 110°16′24″W) is an open-pit operation located on East Island in Lac de Gras, Northwest Territories, Canada (Fig. 1b). The location of the mine is impacted by a subarctic climate with a mean annual air temperature of −4.5 °C. The mine is located on terrain under continuous permafrost with an active thaw zone of approximately 4 m depth (Neuner et al., 2013). The warmest and coldest months are typically July (avg. 16 °C) and January (avg. −27 °C), respectively. The average annual precipitation is 291 mm, and most rainfall occurs between May and October, with ~50% of precipitation falling as snow. Evaporation is approximately 270 mm/yr, occurring predominantly from July to early November (Neuner et al., 2013).

The volcanoclastic and pyroclastic kimberlites pipes of Diavik intrude Late Archean granitoids and supracrustal rocks of the Yellowknife Supergroup in the Slave Structural Province (Graham et al., 1998; Moss et al., 2018). The kimberlites are hosted in moderately to coarsely crystalline peraluminous S-type granites, granodiorites, tonalitic granites, and pegmatites that contain only trace sulfides, resulting in a low potential for acid-generation (Graham et al., 1998; Neuner et al., 2013; Smith et al., 2013). The country rocks contain abundant xenoliths of metasedimentary biotite schist from the Yellowknife Supergroup (Graham et al., 1998). Pyrrhotite [$Fe_{1-x}S$] and minor abundances of other sulfide minerals are locally disseminated in the biotite schist and are potentially acid-generating (Smith et al., 2013). In addition, several Proterozoic diabase dikes are present and correspond to the last intrusive events before kimberlite emplacement (Graham et al., 1998; Smith et al., 2013). The kimberlite pipes are constituted by bedded volcaniclastic kimberlite, and pyroclastic rocks including tuffs, breccias, and mudflows (Graham et al., 1998; Moncur and Smith, 2012). Olivine and serpentine minerals are abundant in the pyroclastic kimberlites (Graham et al., 1998; Moss et al., 2018).

2.2.1. Mineral processing and mine waste management at diavik

Mining operations at Diavik started in 2003 with a production estimated at 2 Mt/yr of kimberlite rock, at an average rate of up to 6300 tonnes of kimberlite per day, mostly mined from an open pit (Smith et al., 2013; Wilson et al., 2009). Gravity-based methods combined with X-ray screening systems are used to separate diamonds from crushed kimberlite rock. After diamond extraction, kimberlite residues are transported as a slurry via a pipeline into a closed basin called Processed Kimberlite Containment facility (PKC). Approximately 2.3×10^6 m^3/yr of water from Lac de Gras has been used in mineral processing (Power et al., 2014). The PKC is a permanent storage facility for two streams of kimberlite residues designated by fine processed kimberlite (FPK) and coarser processed kimberlite (CPK). Until 2016, the PKC was divided into three cells or containment basins, namely: the main closed basin (PKCF) inserted in a natural valley used to store FPK, and the west and southeast cells (CPKC) used to store CPK (Golder Associates Ltd., 2018). CPK has also been used in the construction of containment dams. The CPK is stored subaerially, whereas the PKCF is often flooded with process water, runoff, rain, or snow that falls within the containment area (Wilson et al., 2009). The water collected from a reclaim barge located in the central part of the PKCF pond is used for water quality assessment (Fig. 1b).

In 2006, when Wilson et al. (2009) sampled the processed kimberlite residues, the PKCF had an area of ~0.86 km^2 designed to retain 5–8 × 10^5 m^3 of water (Golder Associates Ltd., 2018). More recently, the PKCF has been expanded and encloses approximately 1.6 km^2 of kimberlite residue storage area (Golder Associates Ltd., 2018). The excess process and runoff water in the PKCF are transferred via a pipeline to the North Inlet, a basin with a storage capacity of 5×10^6 m^3 (Diavik Diamond Mines Inc., 2020). The North Inlet's collects and retains water prior to discharges into Lac de Gras.

2.2.2. Mineralogy of the mine waste

Kimberlite residue sampling by Wilson et al., (2009) was done in September 2005 and August 2006 (Fig. 1b). Efflorescent crusts of secondary minerals were collected from the surface of the mine residues stored in the FPKC. In addition, coring was conducted in the periphery of the PKCF (Fig. 1b), sampling up to 100 cm depth below the surface of the fine PKC. Detailed sampling information is described by Wilson et al. (2009).

The most commonly observed minerals (Table 2) in the kimberlite residues were identified as serpentine minerals [predominantly lizardite: $Mg_3Si_2O_5(OH)_4$; 40.0−76.2 wt%], high−Mg forsterite (Mg_2SiO_4; 12.3−46.3 wt%), calcite ($CaCO_3$; 1.9−4.1 wt%), Cr-rich diopside [$Ca(Mg,Cr)Si_2O_6$], Mg-rich garnets [$(Fe,Mg)_3Al_2(SiO_4)_3$], plagioclase [$NaAlSi_3O_8$], phlogopite [$KMg_3(AlSi_3O_{10})(OH)_2$], quartz ($SiO_2$), and swelling clays (e.g., vermiculite [$Mg_3(Al,Si)_4O_{10}(OH)_2{\cdot}4H_2O$], smectites, and possibly interstratified phases). The evaporative crusts at the surface of PKCF include nesquehonite ($MgCO_3{\cdot}3H_2O$), Ca-carbonates (vaterite, calcite), Na-carbonates {nahcolite ($NaHCO_3$) and trona [$Na_3(NaHCO_3)(CO_3){\cdot}2H_2O$]}, and sulfates [gypsum ($CaSO_4{\cdot}2H_2O$), anhydrite ($CaSO_4$), epsomite ($MgSO_4{\cdot}7H_2O$)] (Wilson et al., 2009, 2011). Radiocarbon results (i.e., $F^{14}C > 1$) are consistent with modern carbon sources (i.e., atmospheric or organic) in secondary carbonates collected from the PKCF (Wilson et al., 2011), providing evidence for storage of atmospheric CO_2 in the processed kimberlite.

2.3. Venetia diamond mine

The Venetia diamond mine (Fig. 1c) is an open-pit operation located 50 km west of Musina, Limpopo, South Africa (22° 25′ 59″ S, 29°18′50″ E). Semi-arid conditions mark the regional climate near the Venetia mine, characterized by high average temperatures (22.4 °C), low rainfall (200–400 mm/yr), and high evaporation rates (2050 mm/yr). Most of the rainfall occurs during summer (October to March).

The kimberlite pipes were discovered in early 1980, and mining operations were initiated in 1993. The pipes are within the Central Zone of the Proterozoic Limpopo Belt and are dominated by either monticellite-phlogopite or phlogopite-calcite assemblages, with the dominant groundmass being serpentine [$Mg_3Si_2O_5(OH)_4$] (Mervine et al., 2018). There are fourteen distinct kimberlite pipes with unique geometry at Venetia. The country rock surrounding the kimberlites is composed of a sequence of amphibolite, quartzo-feldspathic gneisses, biotite gneiss, amphibolite, biotite schist, metaquartzite, and marble (Stripp et al., 2006).

2.3.1. Mineral processing and mine waste management at Venetia

Kimberlite processing results in the annual production of 4.74 Mt of residues (Mervine et al., 2018) that are separated into two streams: ~60% as fine kimberlite residues (<1 mm) and ~40% as coarse kimberlite residues (1−8 mm) after diamond separation by gravity-based methods. The fine residues are stored in two large reservoirs (Fig. 1c), referred to as the Fine Residues Deposits (FRD), that act as retention basins and have a combined area of 3.5 km^2 (Stubbs et al., 2022). The water used in mineral processing is sourced from alluvial aquifers (Greefswald and Schroda wellfields) located near the Limpopo River (Aquatico Scientific, 2016). These waters are transported from the wellfields by a 35 km pipeline into a reservoir inside the mine (i.e., North Dam), where it is stored for further circulation (Aquatico

Scientific, 2016). The waters are characterized by their high salinity that results from the aquifers' low recharge rate and the groundwater age. According to information shared by De Beers Group of Companies, kimberlite processing at Venetia uses ~3.9 × 10^6 m^3/yr of processing water.

2.3.2. Mineralogy of the mine waste

Extensive physical, chemical, and mineralogical characterization of processed kimberlite mine wastes from Venetia have been conducted in recent years — as part Project CarbonVault™ sponsored by the De Beers Group of Companies — to define the potential of kimberlite residues for CO_2 mineralization (Paulo et al., 2021; Stubbs et al., 2022; Zeyen et al., 2022). Fieldwork was conducted in May 2017 and May 2018 on the FRD impoundments. Samples were collected from the surface and at depth in areas of the FRD impoundment that were not flooded (Fig. 1c). In addition, fine kimberlite residues were collected as a slurry from one of the outlet pipes used to transport processed kimberlite into the FRD reservoir. Unprocessed kimberlite rocks were also collected from the ore stockpile and further processed in the laboratory for geochemical and mineralogical analysis. Stubbs et al. (2022) provide further details on sampling procedures.

The kimberlite residues are mineralogically complex and are dominated by serpentine minerals (primarily lizardite); smectite clays [$M^{m+}_{x/m}(Mg_3)(Al_xSi_{4-x})O_{10}(OH)_2{\cdot}nH_2O$, with M, m, and x corresponding to the hydrated interlayer cations, the charge of the M cation, and the layer charge, respectively]; diopside; tremolite [$Ca_2Mg_5Si_8O_{22}(OH)_2$]; and calcite (Paulo et al., 2021; Stubbs et al., 2022; Zeyen et al., 2022). Lizardite is an abundant mineral (10.8−58.4 wt%) and occurs as pseudomorphed forsterite macrocrysts (200 μm −1 cm) and as microcrysts (<200 μm) (Zeyen et al., 2022). Fe– Ca– Mg- and Al-rich smectite (6.2−39.9 wt%) is also abundant and distributed as a fine-grained matrix around the lizardite and calcite microcysts (Zeyen et al., 2022). Potential sources for labile cations in Venetia kimberlite include calcite, diopside, tremolite, and smectite for Ca, and lizardite, diopside, phlogopite, clinochlore, smectite, tremolite, and talc for Mg (Paulo et al., 2021).

Mineral sinks for CO_2 have not yet been identified in the Venetia residues; however, laboratory tests suggest the formation of Ca-, Na-, and possibly Fe-carbonates from the evaporation of porewaters (data not published). Based on the geochemistry of the mine waste, the maximum CO_2 sequestration capacity was estimated at 268–342 kg CO_2/t of kimberlite, assuming full carbonation of the kimberlite and conversion of leached Ca and Mg to carbonates (Paulo et al., 2021). If only the labile component from non-carbonate sources is accessible for CO_2 mineralization, the potential of Venetia kimberlite was estimated at 3–9 kg CO_2/t (Paulo et al., 2021).

3. Geochemical modeling

3.1. Data collection

The water chemistry dataset for Mount Keith was obtained from Wilson et al. (2014). The information available was limited to two water samples, used as input for the model to represent the general chemistry of the pre-processing and tailings (TSF2) waters (Table 3). The dataset covering the water chemistry of Diavik from 2004 to 2005 contained 32 data points selected from the PKCF (N = 16) and the North Inlet (N = 16). These samples covered monthly sampling from February 2004 to September 2005. In this dataset, alkalinity was not reported for the North Inlet. Therefore, hardness was assumed to be equivalent to carbonate ($CaCO_3$) alkalinity in the North Inlet for modeling purposes. Operational data for Mount Keith and Diavik were obtained from Power et al. (2014) and complemented with data obtained from publicly available reports. The annual water consumption (ML of processing water) and ore production (Mt of rock) for both mine sites are reported in Table 1.

Venetia water chemistry and operational data were obtained from internal reports provided by the De Beers Group of Companies for this study. The water chemistry dataset contained 70 water data points recorded between 2009 and 2018 for the pre-processing water (North Dam, N = 35) and the kimberlite waste impoundments (FRD, N = 35). Water sampling frequency at Venetia changed from a monthly (2009–2011) to a quarterly basis from 2012 onwards. In addition, detailed water consumption (m^3/t of rock) and kimberlite processing data (t rock/yr) were provided for the period between 2015 and 2018 by the mine.

The models used values for pH, alkalinity or hardness, temperature, and concentrations of major cations (Ca^{2+}, K^+, Mg^{2+}, Na^+) and anions (Cl^-, NO_3^-, SO_4^{2-}). These parameters were selected for analysis as they are the most relevant to CO_2 sequestration and account for >90% of the analytes in the solution. Changes in these parameters reflect the major dynamics of elements in the waters and mass transfer related to mineral-water reactions and evaporation. Si concentrations were not reported consistently in any dataset; however, these data would be useful in future studies. A summary of the water chemistry for each mine is provided in Table 3. Time-series trends for specific elements in Diavik and Venetia mine waters are also presented in Figs. 2 and 3, respectively. All datasets are included in the mandatory water quantity and quality monitoring programs for the mines, and sampling followed the required standard procedures stipulated by Canadian, Australian, and South African regulations.

Table 3
Summary of the average water chemistry (standard deviation in parentheses) for the mine waste impoundments and processing waters for Mount Keith, Diavik, and Venetia mines.

		Mount Keith		Diavik		Venetia	
	Unit	Source (initial)	TSF2(final)	PKCF(initial)	North Inlet (final)	North Dam (initial)	FRD (final)
		N = 1	N = 1	N = 16	N = 16	N = 35	N = 35
pH		8.2	8.9	9.1 (0.5)	8.1 (0.8)	8.7 (0.5)	8.5 (0.3)
Temp.	°C	n.a.	n.a.	4.0 (4.9)	4.0 (4.4)	n.a.	n.a.
Alkalinity	mg/L	46.0[a]	70.0[a]	99.8[a] (23.9)	144.2[b] (22.4)	175.6[a] (36.7)	129.4[a] (41.3)
Ca	mg/L	385.0	100.0	11.0 (5.3)	20.5 (4.7)	25.5 (48.3)	51.2 (62.7)
Mg	mg/L	2600.0	1600.0	26.7 (11.0)	20.8 (3.3)	21.9 (8.1)	21.7 (16.9)
Na	mg/L	19000.0	15000.0	38.0 (7.1)	38.2 (7.1)	158.0 (128.8)	979.1 (489.7)
K	mg/L	1200.0	870.0	41.1 (8.2)	13.0 (2.4)	9.6 (6.5)	95.0 (63.0)
Cl	mg/L	32000.0	23000.0	27.5 (7.6)	79.2 (19.5)	136.2 (91.2)	809.9 (411.9)
NO_3^-	mg/L	50.0	20.0	9.0 (3.3)	7.9 (1.8)	2.6 (5.3)	36.6 (31.3)
SO_4^{2-}	mg/L	9200.0	8400.0	110.9 (5.1)	14.0 (5.1)	144.4 (136.1)	996.7 (646.4)

n.a. − information not available.
[a] HCO_3^-.
[b] $CaCO_3$.

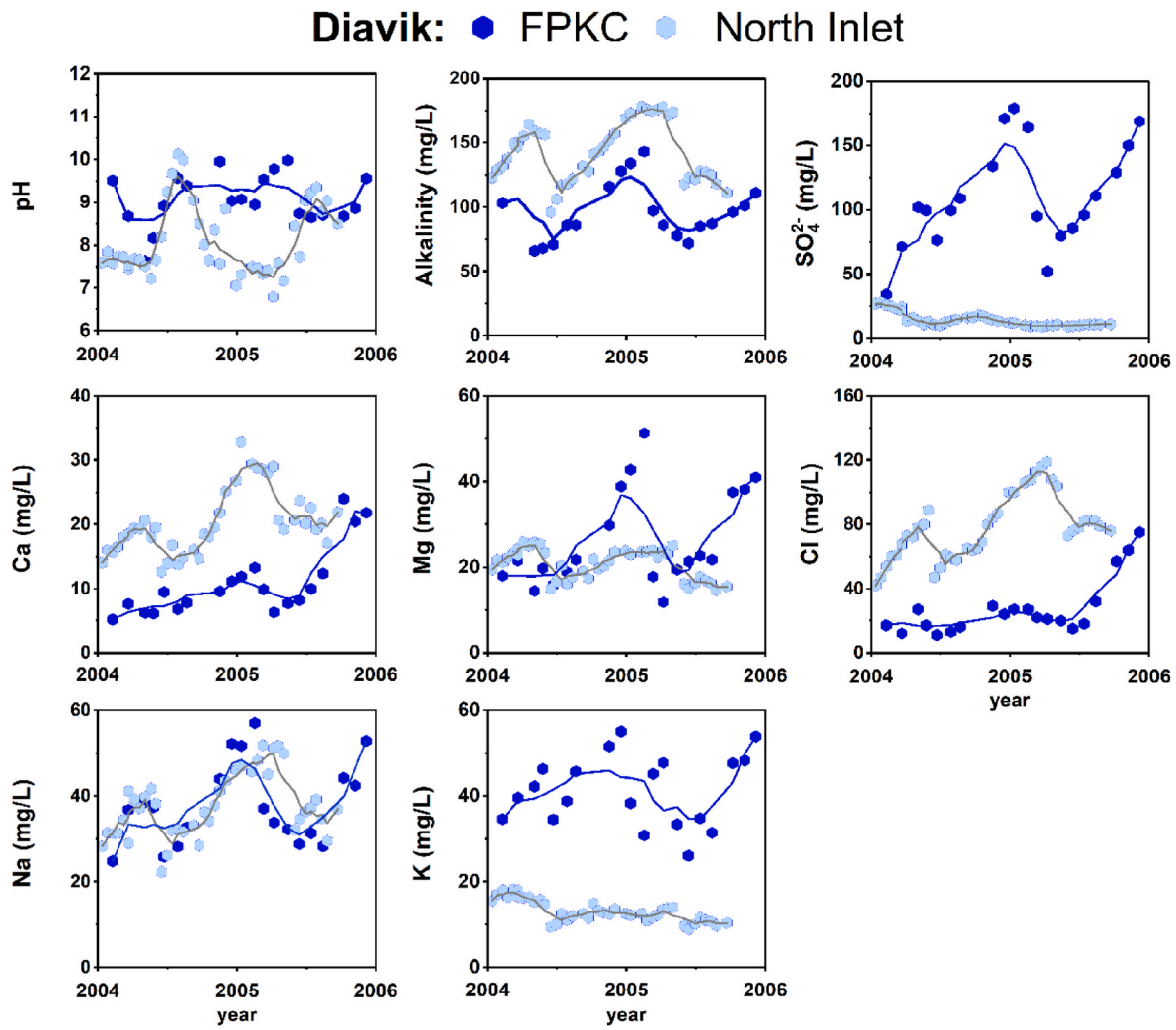

Fig. 2. pH, alkalinity (mg/L), and major ion concentrations (mg/L) in Diavik mine waters. Lines represent the 5-day moving averages for each element in the PKCF (blue dots and line) and the North Inlet (light blue dots and gray line) waters.

3.2. Prediction of secondary carbonate minerals saturation

Mineral trapping of CO_2 in mine wastes is driven by partial or complete evaporation of porewaters (Power et al., 2013). PHREEQC (Parkhurst and Appelo, 2013) was used to simulate evaporation and to predict whether secondary carbonate minerals are saturated in the mine waters. As Parkhurst and Appelo (2013) describe, the evaporation model simulates an irreversible reaction where water is continuously lost from the chemical system. In this model, a volume of tailings water (1 L) was concentrated by sequentially removing a fixed amount of water. The *pitzer. dat* database was preferred for simulations because the specific-ion-interaction model of Pitzer provides more accurate predictions of mineral equilibria in high ionic strengths ($I > 1$) conditions compared to other geochemical databases (Lu et al., 2022a; Parkhurst and Appelo, 2013), particularly under high evaporation conditions. The concentration factors were determined by the quotient between the volume of the initial and final water and after evaporation. Ca- and Mg-carbonate minerals were compared before and after evaporation, and changes in SI were used to indicate viable conditions ($SI > 1$) for their precipitation. For simplification, evaporation was simulated at a constant temperature of 25 °C and not in equilibrium with atmospheric pCO_2 ($10^{-3.4}$ atm). Phases were not removed after saturation in waters, as this did not show that hydrated-Mg carbonates became saturated, despite their presence in tailings. With our simulations, we do not explore the precipitation reactions or sequential removal of minerals from the solution. Instead, we provided an indirect approach to validate the field data and identify the secondary carbonate minerals, including hydrated Mg-carbonate, that are more likely to precipitate in tailings and act as CO_2 sinks for mass-balance models.

3.3. Inverse modeling

The objective of the numerical method of inverse modeling was to determine the set of mole transfers for specific mineral and gas phases (e.g., CO_2) that result in chemical changes along a defined flow path correlated to mineral carbonation reactions. For each mine, the flow paths were defined between a selected initial and final sampling locations used in water quality monitoring programs. The initial and final locations were set preferentially before and after mineral processing or slurry deposition, respectively (Fig. 1, Table 3). As such, the flow paths were defined as: (1) from the source water (Albion borefields) to the TSF2 at Mount Keith; (2) from the PKCF to the North Inlet at Diavik, and (3) from the North Dam (source) to the FRD at Venetia (Fig. 1). The mineralogical data for each site were obtained from previous studies (Paulo et al., 2021; Stubbs et al., 2022; Wilson et al., 2009, 2014).

The mass-balance models with the inverse modeling function were developed using PHREEQC V3 (Parkhurst and Appelo, 2013) and the *carbfix. dat* thermodynamic database (Voigt et al., 2018). This database has been optimized for CO_2–water–mineral reactions, including most of the minerals present in the mine wastes and their reactions with CO_2,

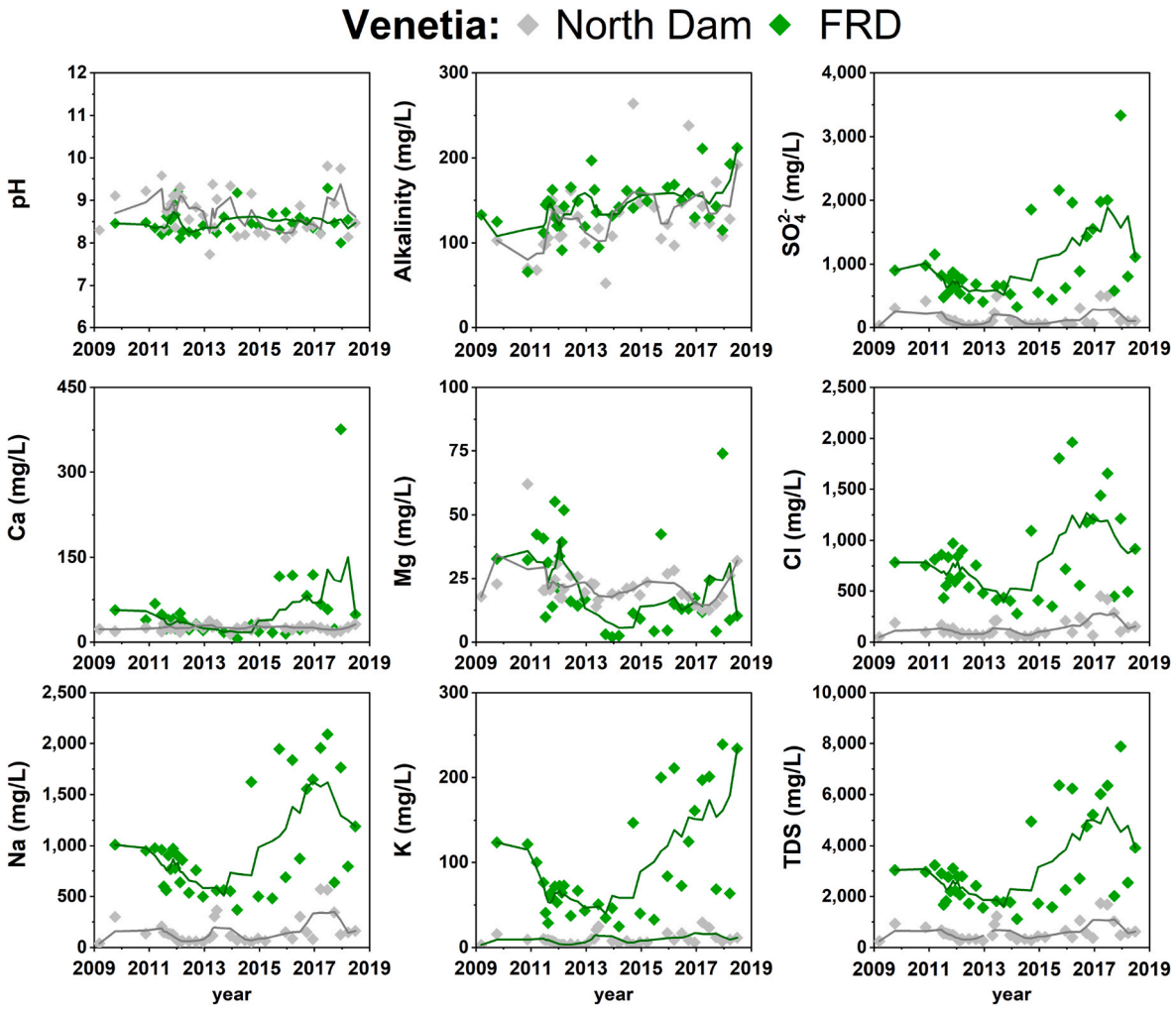

Fig. 3. pH, alkalinity (mg/L), and major ions concentrations (mg/L) in Venetia mine waters. Lines represent the 5-day moving averages for each element in the North Dam (gray) and the FRD (green) waters.

except for some secondary carbonate minerals. As such, the thermodynamic data for hydromagnesite (Gautier et al., 2014), nesquehonite and dypingite (Harrison et al., 2019), and trona (Ball and Nordstrom, 1991) were added to the model input. A set of minerals was constrained to precipitate, or dissolve based on their solubility products. For example, silicate minerals and brucite (*i.e.,* Mount Keith model) were set to dissolve, whereas calcite was allowed to function as either an ion source (dissolve) or sink (precipitate). Although dolomite and magnesite were found to be oversaturated (SI > 1) in the mine waters, when present, these phases were only set as ion sources (dissolution) because their precipitation is kinetically inhibited at Earth's surface conditions (Arvidson and Mackenzie, 1999); therefore these minerals are unlikely to precipitate directely from the mine waters. More common low-temperature precipitates, such as hydrated Mg-carbonates (hydromagnesite, nesquehonite, dypingite) and Na-carbonates (trona, nahcolite), sulfates (gypsum), and amorphous SiO_2 were set to precipitate. Mg-sulfates were not included in the model because these are less abundant and not saturated in waters. Cation exchange (CaX_2, NaX, MgX_2, KX, where X corresponds to the exchange master species) was also introduced in the diamond mine models due to the high abundance of smectites in the kimberlite, which can serve as a source of cations for carbonation reactions (Zeyen et al., 2022).

Data for mass-balance calculations can be affected by analytical errors, spatial or temporal variability in the concentration of each element, alkalinity, and fraction mixing. These unknowns are constrained by an uncertainty limit that fixes the maximum deviation of the concentration of an element allowed for the mass-balance calculations (Parkhurst, 1997; Parkhurst and Appelo, 2013). Satisfying the mass, valence, and charge balances in simulations was obtained for uncertainty limits of 0.5–0.8 (±50−80%). These limits assumed a larger variation of the concentration of each element in the solution to produce viable models (Murray et al., 2021; Parkhurst and Appelo, 2013). Increasing the uncertainty limits also helped reduce the number of reactions predicted by models (Parkhurst, 1997) and simplified the analysis for possible carbon removal pathways in the mine waste impoundments. Due to the multiple mass-balance simulations generated, a set of criteria was defined to better scrutinize the model predictions. First, the output data were scrutinized to reject: (i) all simulations that predicted the precipitation of silicate minerals (e.g., lizardite, forsterite, diopside) or showed results inconsistent with minerals stability; (ii) all simulations with a residual sum of squares greater than 5 (RSS>5) were rejected to limit the analytical data being changed by their maximum uncertainty, and (iii) results that produced mole transfer values greater than 1 mol/L for CO_2 were not selected as these often resulted from a larger mole transfer contribution from the dissolution of silicate minerals (>1 mol/L) when compared to carbonate and sulfate minerals, which dissolution is in general three orders of magnitude faster than silicate (Power et al., 2013). Scenarios with large moles transfer produced unrealistic estimates of CO_2 consumption (mega to gigatonnes) at low temperature and pressure conditions, and therefore were discarded. Once these models were removed, the remaining models were sorted according to scenarios dominated by the dissolution of specific minerals (e.g., forsterite,

lizardite, brucite, calcite). The mole transfer for CO_2 for the viable scenarios were averaged and the mine passive carbonation rate (R) was determined with the general formula (Eq. 1), where mCO_2 corresponds to the average CO_2 mole transfer per liter of solution, M_{CO2} is the molar mass of CO_2 (g/mol), A corresponds to the area (m^2) of the mine waste impoundments, and V is the volume of water (L/yr) used in mineral processing per year. This operation was repeated for each sampling period listed in the mine water chemistry data.

$$R\left(g\,/\,m^2\,/\,yr\right) = mCO_2 \times M_{CO2} \times [1\,/\,A] \times \mathrm{V} \quad (1)$$

Calculations for Mount Keith and Diavik used constant volumes of processing water (L/yr) reported in Table 1. For Venetia, the calculations between 2009 and 2014 use a fixed processing water volume of 3×10^6 m^3/yr, whereas the rate calculations from 2015 to 2018 incorporated the specific volumes recorded by the mine as part of their monthly monitoring programs. Because the Venetia dataset also covered multiple years, the mass of CO_2 consumed between specific time intervals could be calculated by a definite integral (Eq. (2)) that calculates the area (m_{CO2}) under the passive carbonation function $R(t)$ for the interval (years) $a \le x \le b$.

$$m_{CO2}\ \left(g\ CO_2\,/\,m^2\right) = \int_a^b R(t)dt = \lim_{n\to+\infty} \sum_{k=1}^{n} R(t)t \quad (2)$$

4. Results and discussion

4.1. General physicochemical characteristics of the mine waters

Waters from the three mines have an alkaline pH > 8 (Table 2) and high electrical conductivity (EC). TSF2 waters at Mount Keith have a pH ~8.9, whereas the pH of the source water has been measured at 8.2 (Table 2). At Diavik, the average pH in PKCF waters has been recorded at 9.1 ± 0.5, and a slightly lower pH is recorded for the North Inlet (8.1 ± 0.8). Time series data (Fig. 2) also showed that the pH of the North Inlet waters fluctuates more widely during spring and summer months than in the PKCF (Fig. 2). These fluctuations are possibly related to seasonality (i.e., ice thawing, increased runoff) and periods of water discharge from PKFC to the North Inlet. At Venetia, the average pH values of the source water (North Dam) and the FRD waters are 8.7 ± 0.5 and 8.5 ± 0.3, respectively. However, the pH of the North Dam waters experiences greater fluctuations when compared to those in the FRD (Fig. 3).

Greater EC values were reported for Mount Keith waters (110,000 μS/cm), followed by waters from Venetia (North Dam: 479−2800 μS/cm; FRD: 1890−9770 μS/cm), and Diavik (PKCF: 381−920 μS/cm; North Inlet: 342−700 μS/cm) attesting their saline composition. The average elemental concentrations (Table 3) indicate that ion predominance in Mount Keith waters follows the sequence $Cl^- > Na^+ > SO_4^{2-} > Mg^{2+} > K^+ > Ca^{2+} > NO_3^- > Mg^{2+} > HCO_3^-$. At Diavik, sulfate is the most predominant ion in PKCF waters ($SO_4^{2-} > HCO_3^- > K^+ > Na^+ > Cl^- > Mg^{2+} > Ca^{2+} > NO_3^-$), whereas bicarbonate is more dominant in the North Inlet ($HCO_3^- > Cl^- > Na^+ > Mg^{2+} > Ca^{2+} > SO_4^{2-} > K^+ > NO_3^-$). The FRD waters from Venetia follow a similar trend with sulfate as the most abundant ion in the residues ($SO_4^{2-} > Na^+ > Cl^- > K^+ > HCO_3^- > Ca^{2+} > NO_3^- > Mg^{2+}$) versus the North Dam waters where sodium is more dominant ($Na^+ > SO_4^{2-} > Cl^- > HCO_3^- > Ca^{2+} > Mg^{2+} > K^+ > NO_3^-$). The ionic charge balance for most samples was ≤10% suggesting that the major ions species in solution were well-balanced and that the mine water chemistry datasets used for geochemical modeling were reliable.

Mount Keith waters have the greatest dissolved solids concentrations for the ultramafic mines under evaluation, except for alkalinity, which was greater at Venetia (Table 3). For example, the Mg concentration in TSF2 is recorded at 1600 mg/L versus 100 ± 24 mg/L and 175 ± 37 mg/L in Diavik (PKFC) and Venetia (FRD), respectively. The concentration of Ca^{2+} in TSF2 is expected to be low since mineral sources for this element are scarce in Mount Keith mine residues. However, the concentration of 100 mg/L of Ca^{2+} in TSF2 is still greater than those reported for the diamond mines (11 ± 5 mg/L PKCF; 51 ± 63 mg/L FRD). Cl^- and Na^+ concentration in Mount Keith waters are 30–300 and 15–370 orders of magnitude greater than the measured concentrations of the same elements in Diavik and Venetia waters (Table 3). Sulfate concentrations of 8400 mg/L in TSF2 largely exceed those measured in the diamond mines residue impoundments, which typically contain 10 to 100 times less SO_4^{2-}. Likewise, K^+ concentrations are 6–70 times greater at Mount Keith than at the diamond mines (Table 3). In contrast, the alkalinity of Mount Keith waters (<70 mg/L) is the lowest recorded (Table 3).

At Diavik, long-term water quality trends (Fig. 2) show that Cl^- concentrations in PKCF remained relatively constant until mid-2015 (Fig. 2). After this period, Cl^- concentrations steadily increased from 20 mg/L to 80 mg/L. Ca^{2+} shows a similar trend to Cl^- suggesting that these elements varied together (Fig. 2), possibly due to evapoconcentration. Changes in alkalinity, Mg^{2+}, SO_4^{2-}, K^+, and Na^+ in the PKCF (Fig. 2) follow an undulated trend, likely affected by seasonality, with greater concentrations peaking during the winter months. This trend appears to be independent of the Cl^- pattern, suggesting that evapoconcentration has less impact on alkalinity, Mg^{2+}, SO_4^{2-}, K^+, and Na^+ variations. A similar undulated trend was observed for all elements in the North Inlet (Fig. 2). Concentrations of Ca^{2+}, Cl^-, and alkalinity in the North Inlet are systematically greater than in the PCKF, whereas Mg^{2+}, K^+ and sulfate concentrations are much lower in the North Inlet (Fig. 2). Na concentrations are similar in PKCF and North Inlet waters.

The water chemistry of the North Dam at Venetia mine has been relatively stable over the nine-year period. Conversely, the concentrations of Ca^{2+} and Mg^{2+} in the FRD have increased at least two times for the same period (Fig. 3). The trends of Ca^{2+}, Mg^{2+}, Na^+, K^+, and SO_4^{2-} concentrations converge with those observed for conservative elements (e.g., Cl^-), suggesting that these elements are under a similar environmental influence, and that most likely their concentrations in the mine residues impoudment are regulated by evapoconcentration of the waters and, consequently mineral precipitation. Evapoconcentration of the FRD waters can be expected to range from 5 to 30 times based on the difference in the concentration of Cl^- in the North Dam and the FRD. From 2012 to 2015, Ca^{2+} and Mg^{2+} were not evapoconcentrated in the FRD, and concentrations were lower than those measured in the North Dam (Fig. 3). In contrast, the concentration of Cl^- increased by approximately five times during the same period. These data indicate that there is a sink for Ca^{2+} and Mg^{2+} in the kimberlite wastes, such as carbonate and/or sulfate minerals. After 2015, the concentrations of Ca and Mg in the FRD have increased and fluctuated more often, closely matching variations in Cl^- concentration. Mineral dissolution and precipitation cycles may have significantly influenced the FRD water chemistry after 2015. Recirculation and dewatering of the FRD are also likely to have affected the water quality during this period. All cations and anions concentrations in the FRD have increased after 2015. Alkalinity has increased consistently in the North Dam and FRD waters from 2009 to 2015 (Fig. 3).

A Piper diagram was used to classify the predominant hydrochemistry types for waters from each mine (Fig. 4). Mount Keith waters were classified as sodium−chloride−sulfate-type waters (Fig. 4). The PKCF waters from Diavik were defined as predominantly SO_4^{2-} type waters, whereas the waters from the North Inlet were characterized as mixed HCO_3^- and Cl^- type waters. Venetia waters were classified as Cl−type with a predominance of Na^+ and K^+. The high SO_4^{2-} and Cl^- in the mine waters suggests that evaporation strongly affects the water chemistry. The enrichment in SO_4^{2-} and Cl^- is more prevalent at Mount Keith and Venetia because of their arid climate conditions where annual evaporation (>2000 mm) is greater than precipitation (Table 1). Nevertheless, the PKCF at Diavik is also affected by evapoconcentration, as suggested by the predominance of SO_4^{2-} and Cl^- type waters, the long-term increasing trend of Cl^- concentrations in the waters (Fig. 2), and *in-*

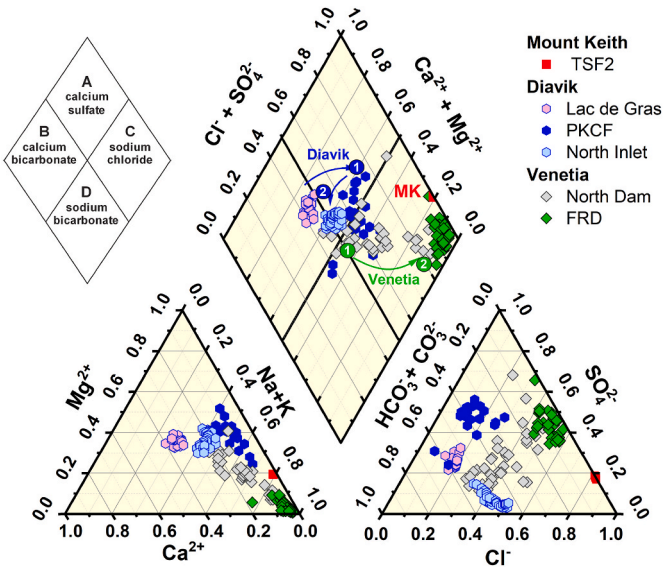

Fig. 4. Piper diagram showing the main water chemistry-type for Mount Keith (MK), Diavik, and Venetia waters. Mount Keith and Venetia waters are dominated by Na–Cl type waters, whereas Ca–SO_4 dominates at Diavik. The arrows indicate the general water path used for modeling. Values for ions concentration are in meq/L.

situ precipitation of sulfates reported by Wilson et al. (2011). Due to limited storage capacity, the PKCF impoundment is frequently drained and discharged into the North Inlet. As a result, the discharge contributes to the export of ions and alkalinity from PKCF to the North Inlet (Fig. 2). This practice exposes kimberlite residues to drier conditions in the PKCF, which can lead to the precipitation of secondary carbonate minerals on their surface leading to the formation of the efflorescences reported by Wilson et al. (2009).

At Venetia, mine wastes are deposited as slurries in the impoundments that first react with process waters and are further weathered when exposed to rainfall. Weathering of mine residues is influenced by the composition of waters used for ore processing and depends strongly on climate. The majority of the water used by the plant is recirculated for mineral processing in a closed loop. However, the slurries deposited on the FRD retain their water and, for that reason, dissolved ions in the water retained by the FRD are expected to become more concentrated due to evaporation, which is conducive of the precipitation of secondary minerals. The progressive increase of Ca^{2+}, Na^{+}, K^{+}, Cl^{-} concentrations and alkalinity in the Venetia residues waters over nine years is likely a consequence of the combined effects of continuous deposition of kimberlite slurries, water mixing, and the evapoconcentration cycles that affect water chemistry (Fig. 3). Yet, this trend was not observed for Mg, whose concentration has generally decreased from 2009 to 2016 in the mine waste impoundment waters, which can be related to silicate weathering.

4.2. Determining mineral sinks for CO_2 with geochemical modeling

Results from evaporation simulations and their effect on secondary mineral saturation indices (SI) in mine residues impoundments waters are presented in Fig. 5. Waters from Mount Keith are initially slightly saturated with respect to calcite (SI = 0.25) and undersaturated in hydrated Mg-carbonates (hydromagnesite, nesquehonite, dypingite, SI < 0), gypsum (SI < 0), and epsomite (SI < 0). With gradual water evaporation, calcite saturation was predicted to increase further until it plateaus at SI ≈ 1 in the TSF2 at approximately a 10−fold concentration factor. Afterward, calcite saturation drops, and gypsum becomes supersaturated. Hydromagnesite and dypingite become saturated once more than 40% of the water in the TSF2 evaporate (>3−fold

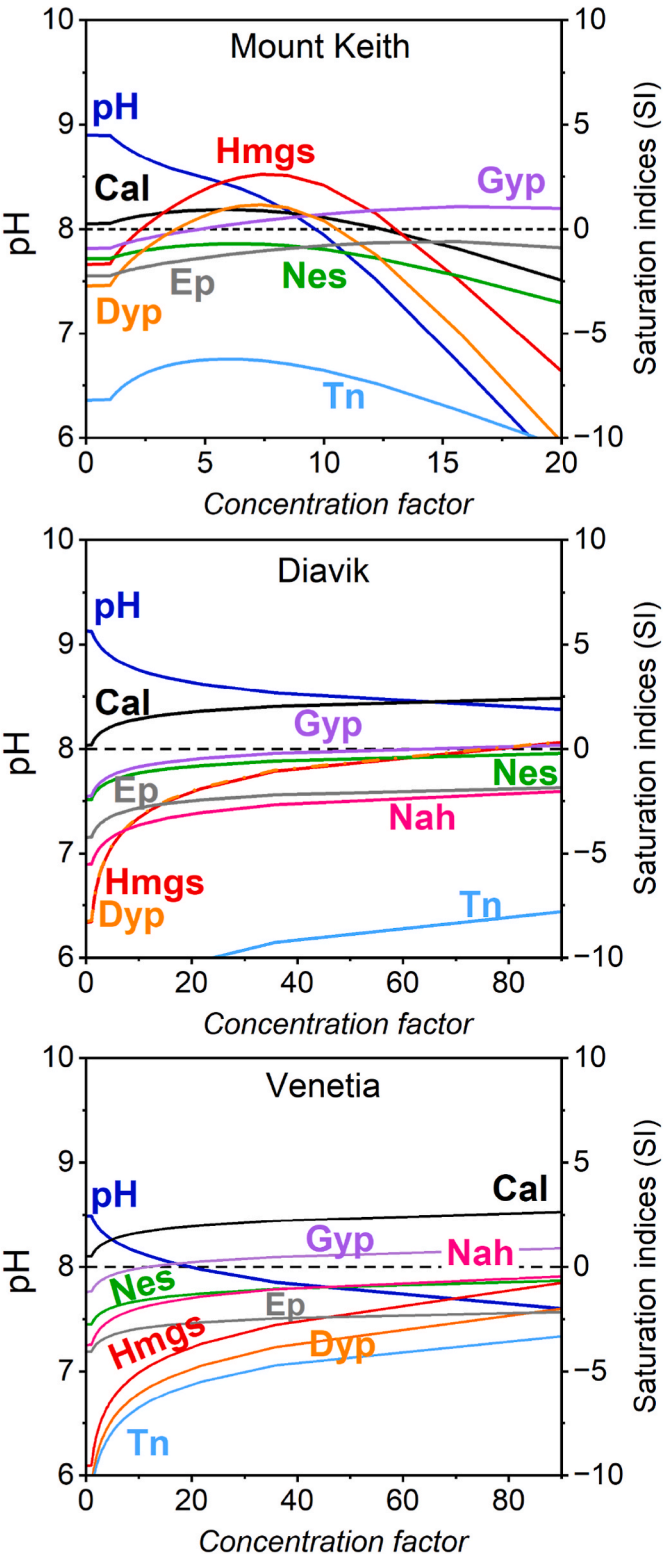

Fig. 5. Simulations of the effect of evaporation on minerals saturation indices (SI) in the mine waste impoundment waters. The evaporation simulations indicate that calcite is saturated in all mine waters and can precipitate, whereas hydrated Mg-carbonate minerals are more likely to precipitate from Mount Keith and Diavik waters (PKCF). Concentration factors represent the quotient between the initial mass of water and the mass of water after evaporation (*i.e.*, after moles removal). Nesquehonite, Na-carbonate minerals, and gypsum require greater concentration factors to reach saturation. Minerals identified in the model include Cal – calcite, Gyp – gypsum, Hmgs – hydromagnesite, Nes – nesquehonite, Dyp – dypingite, Tn – trona, Nah – nahcolite, Ep – Epsomite.

concentration factor). The simulations show that after carbonate saturation, the rapid pH decrease predicted for TSF2 is consistent with carbonate precipitation scenarios. Nesquehonite remains undersaturated in the Mount Keith waters, even if evaporated, and therefore unlikely to be a sink for CO_2 in the mine wastes. Trona and epsomite remained undersaturated in Mount Keith waters even at greater concentration factors.

Evaporation of the kimberlite mine waters results in an abrupt pH decrease (Fig. 5), which is consistent with carbonate mineral precipitation. Calcite is saturated in the PKCF waters at Diavik (SI = 0.2), and applying a ten-fold concentration factor, the SI rises to ≈1.4, which strongly suggests calcite as a viable sink for CO_2. Diavik waters are generally undersaturated with respect to hydromagnesite, nesquehonite, and dypingite. However, increasing evaporation of the waters results in hydromagnesite, dypingite, and nesquehonite reaching SI values closer to saturation in the PKCF, which can lead to mineral trapping of CO_2 if these minerals can precipitate. Wilson et al. (2011) reported that nesquehonite is the most common secondary Mg-carbonate in the Diavik fine residues. Nesquehonite occurs as thin efflorescences at the surface and is also preserved at trace abundance (<1 wt%) in deeper residues (Wilson et al., 2011). Transformation of nesquehonite to either dypingite or hydromagnesite occurs at temperatures greater than 25 °C. Furthermore, the direct precipitation of hydromagnesite is kinetically inhibited below 40 °C. These temperatures are rarely exceeded at Diavik; hence Mg-carbonate transformations are likely slowed (Harrison et al., 2019; Power et al., 2009; Wilson et al., 2011), which may explain the absence of dypingite and hydromagnesite in the tailings despite having SI > 0 as a result of evaporation. Nesquehonite reaches saturation only after nearly complete evaporation of PKCF waters, providing an explanation for its relative scarcity and predominance in drier areas of the PKCF. Epsomite and the sodium carbonates remained undersaturated. Gypsum and Na-carbonates were more frequently observed in tailings than Mg-sulfates (Wilson et al., 2011).

Venetia mine waters are slightly supersaturated with respect to calcite (SI_{cal} = 0.5−0.7) and become rapidly more supersaturated (SI_{cal} ≈ 1.6) above a 10−fold evapoconcentration (Fig. 5). Gypsum saturation index (SI_{gyp}) reaches values greater than zero in the FRD waters with a 20−fold evaporation. Thus, the precipitation of calcium sulfate minerals in FRD may interfere with CO_2 mineralization at Venetia by reducing the Ca available to form calcium carbonates. Hydrated Mg-carbonate minerals have not been found in the Venetia mine residues, and the model corroborates that these minerals will remain undersaturated even after extensive evaporation. Moreover, the Mg/Ca molar ratio of ~0.4 will not inhibit calcite precipitation (Mg/Ca >2) in favor of the precipitation of aragonite and Mg-carbonates (Sun et al., 2015). Therefore, calcite is likely the main secondary carbonate phase forming in the mine waters.

The predicted mineral sinks for CO_2 are consistent with mineralogical data from previous studies of the Mount Keith and Diavik mines waste (Wilson et al., 2009, 2011, 2014). Based on geochemical modeling, the most viable sinks for mineral trapping are calcite and hydromagnesite for Mount Keith; calcite, nesquehonite, dypingite, and hydromagnesite for Diavik (PKCF); and calcite for Venetia (FRD) (Fig. 5). Nesquehonite and sodium carbonates (e.g., trona and nahcolite) also form in the kimberlite mines and have been previously documented in efflorescences at Diavik, instead of dypingite and hydromagnesite for which formation is inhibited by the low temperatures. However, nesquehonite, trona, and nahcolite saturation require close to complete evaporation of mine waters. Mg-sulfates, like epsomite, are also not saturated in the mine water even at high evaporation and tend to redissolve as tailings are rewetted.

Although Mount Keith and Diavik waters are also saturated with respect to dolomite and magnesite (SI > 1), their formation at Earth's surface conditions is very slow (Power et al., 2019). For this reason, dolomite and magnesite were not considered viable sinks for CO_2 and, therefore, not reported in the modeling results and were not considered sinks for inverse modeling. In fact, the greater saturation of dolomite, magnesite, and huntite in the models compared to the hydrated Mg-carbonates, became a limitation to determine the potential CO_2 sinks in tailings. For example, dolomite, magnesite, and huntite were rapidly saturated at lower concentration factors but not the hydrated Mg-carbonate. If the simulations had considered removing dolomite, magnesite, and huntite by precipitation as these became saturated, the hydrated Mg-carbonates could not saturate in the remaining waters containing much lower alkalinity and cations concentrations, despite evidence of their occurrence in the mine tailings. As such, the evaporation models were conducted without mineral removal by precipitation to detect the possible carbon sinks that can form from saturated mine waters. This approach is intended to determine the potential CO_2 sinks at ambient temperatures rather than mimicking sequential mineral precipitation reactions in the mine tailing waters.

Waters from all three mines were saturated with respect to calcite, regardless of the amount of evapoconcentration that was modeled. Hence, secondary calcite will likely form in all types of ultramafic mine wastes evaluated. Since calcite is commonly present as a bedrock or gangue mineral in ultramafic ores, validating the presence of secondary calcite in mine wastes cannot be easily assessed through crystallographic assessments. Geochemical modeling provides complementary information for understanding reaction pathways and CO_2 sinks in mine wastes.

4.3. Passive carbonation rates

4.3.1. Mount Keith nickel mine

Wilson et al. (2014) estimated the initial brucite content in Mount Keith tailings at 2.5 wt%. Although brucite is usually a minor phase of ultramafic rocks, its dissolution is orders of magnitude faster than the more abundant silicate minerals (Harrison et al., 2013; Power et al., 2013). For this reason, mine wastes containing brucite have greater reactivity to CO_2 at ambient conditions and, consequently, a more significant potential to offset carbon emissions (Assima et al., 2013b, 2014; Beaudoin et al., 2017; Paulo et al., 2021; Power et al., 2020). The reaction of brucite with CO_2 to form hydromagnesite (Eq. (3)) was determined with inverse modeling to be the dominant process affecting changes in Mount Keith water chemistry (Table 4).

The model results corroborate Wilson et al. (2014), who determined the passive carbonation rate at Mount Keith based on the measured abundance of hydromagnesite in tailings. The viable models that predicted the consumption of CO_2 through brucite carbonation did not include serpentine minerals dissolution predictions. When simulated, lizardite dissolution was predicted to exceed the 1 mol CO_2/L threshold

Table 4
Mount Keith passive sequestration rates calculated from geochemical mass-balance modeling (scenario 2). The moles transferred were used to calculate the mass of CO_2 linked to brucite carbonation in TSF2. Phases that dissolved are presented as positive (+) values, and phases that precipitated as negative (−) values.

Phases	mol/L	g CO_2/L	t CO_2/yr	Passive carbonation rate g CO_2/m^2/yr
CO_2(g)	1.57×10^{-1}	6.89	65,701	3958
Lizardite	n.c.			
Dolomite	n.c.			
Calcite	-7.62×10^{-3}	−0.34	−3198	−192
Hydromagnesite	-3.79×10^{-2}	−6.66	−63,511	−3826
Brucite	1.97×10^{-1}	6.94	66,136	3984
SiO_2(am)	n.c.			
Gypsum	-1.03×10^{-2}			
Magnetite	n.c.			

n.c. − no change.

defined as criteria to reject simulations scenarios as these produced an overestimated CO_2 consumption rate (Mt to Gt). In addition, most simulations with lizardite dissolution were uncoupled with the consumption of CO_2 and, therefore, discarded from the analysis. Wilson et al. (2014) reported that despite observing that serpentine minerals can act as seeds for hydromagnesite crystals in Mount Keith tailings, their contribution to CO_2 sequestration at Mount Keith is likely minimal compared with brucite carbonation. These authors have shown that brucite abundance declines in all surficial tailings (<25 cm) while it is accompanied by an almost proportional increase of hydromagnesite in the tailings. In contrast, the changes in serpentine abundance in the tailings are likely reflecting a dilution effect in Rietveld refinement estimates introduced by adding new crystalline mass (i.e., precipitates) to the tailings rather than by extensive weathering of serpentine. Furthermore, laboratory carbonation experiments indicated that brucite dissolution is viable at near-ambient pressures and temperatures in alkaline brines, similar to the Mount Keith tailings water (Harrison et al., 2015). Finnaly, reactive transport modeling simulations corroborated the development of a brucite-depleted zone linked to the precipitation of hydromagnesite, whereas serpentine dissolution is unlikely to occur under the supersaturated conditions of the tailings waters {Wilson et al., 2014 #3}. Thus, despite the 49–90 wt% abundance of serpentine minerals (lizardite, antigorite, and minor chrysotile), lizardite dissolution contribution for CO_2 sequestration was considered minimal for our model.

$$(OH)_2 \;\; 4CO_2 + H_2O \;\; Mg_5(CO_3)_4(OH)_2 5H_2O \tag{3}$$

The relative stoichiometry derived from inverse modeling for brucite to CO_2 molar ratio (1.254) agrees with the expected molar ratio of 1.25 for brucite to CO_2 in carbonation reactions (Table 4). Therefore, Mount Keith's most plausible CO_2 sequestration scenarios involve brucite carbonation accompanied by either calcite dissolution (scenario 1) or calcite precipitation (scenario 2; Table 4). Mineralogical data presented by Wilson et al. (2014) show that calcite abundance remains relatively constant (<0.5 wt%). Moreover, Mount Keith waters are saturated relative to calcite (Fig. 5), and the pH > 8 (Table 3) favors carbonate precipitation rather than dissolution. Thus, scenario 2, for that reason, is more likely to occur as part of the CO_2 mineralization reactions in Mount Keith.

The mass of brucite added yearly to the mine waste impoundments was computed from the annual tailings production (11 Mt) and the average abundance of brucite (2.5 wt%). The tailings impoundments were estimated to have received ~275,000 t $Mg(OH)_2$ per year. The complete carbonation of this brucite (Eq. (3)) would sequester ~166,000 t CO_2/yr as hydromagnesite. However, brucite carbonation is limited by the slow ingress of CO_2 into tailings and only 55 wt % or ~151,000 t of t $Mg(OH)_2$ were estimated to react in tailings (Wilson et al., 2014). In our model, the brucite carbonation reaction was estimated to consume ~1.6×10^{-1} mol/L of CO_2 or ~7 g of CO_2 per liter of process water (Table 4). Given that 9534 ML of water were expected to interact with the tailings annually, the mass of CO_2 consumed by brucite carbonation was estimated at ~66,000 t CO_2/yr, meaning that ~109,000 t/year of brucite would be carbonated in the tailings. These values correspond to the carbonation of ~40% of the total mass of brucite added to the tailings, which resembles the conclusions of Wilson et al. (2014). Mineral trapping as hydromagnesite was calculated at ~63,500 t CO_2/yr, which is equivalent to a passive carbonation rate of ~3960 g CO_2/m^2/yr (Table 4). For comparison, the passive carbonation rate estimated with QXRD using 172 tailings samples collected from TSF2 and based on hydromagnesite abundance was determined at 2400 g CO_2/m^2/yr or ~40,000 t CO_2 per year (Wilson et al., 2014). Overall, our model predictions are consistent with these rates demonstrating the practicality of using inverse modeling as a tool to determine passive carbonation rates for active mines.

4.3.2. Diavik diamond mine

Mass-balance simulations using the PKCF and North Inlet waters predicted that the dissolution of silicate and carbonate minerals affect passive carbonate rates. Viable scenarios (Supplementary Table A) for CO_2 mineralization were dominated by the dissolution of lizardite (scenario D1) and forsterite (scenario D2). These scenarios included calcite dissolution and the precipitation of Na-carbonates, amorphous SiO_2, and gypsum as the most abundant secondary minerals (Table 5). Scenarios that predicted nesquehonite precipitation were not considered for analysis as these simulations failed to fit the validation criteria defined for the inverse model predictions (e.g., CO_2 and nesquehonite mole transfer >1). Furthermore, dypingite and hydromagnesite were not predicted to form.

The average Si concentration in the PKCF waters (~2.3 mg/L; n = 2) is two orders of magnitude greater than in the Lac de Gras waters (~0.01 mg/L; Deton' Cho Stantec (2015)), which are used for ore processing. The range of amorphous SiO2 mole transfer predicted for scenarios D1 (−1.2 × 10−4 to -6.1×10^{-4} mol/L) and D2 (-1.1×10^{-4} to -4.9×10^{-4} mol/L) corresponds to a dissolved load of 8 ± 4 mg Si/L and 1 ± 0.4 mg Si/L, respectively. These values are in good agreement with field results and support the link between silicate weathering and CO_2 sequestration for Diavik, as reported by Wilson et al. (2011). Nevertheless, the acid neutralization potential (NP) of the kimberlite residues was estimated at ~39–85 kg $CaCO_3$ eq/t, and primarily regulated by calcite dissolution (Moncur and Smith, 2012). Carbonate dissolution would be promoted by the slightly acidic waters of Lac de Gras (pH: ~6.6; $SI_{Calcite} < 0$) used for kimberlite processing and cause an increase in dissolved inorganic carbon that is not related to silicate dissolution.

Since calcite dissolution (Eq. (4)) was predicted for all the viable scenarios, the passive carbonation rate is potentially affected by the recycling or loss of stored carbon from the residues. In fact, the secondary Ca- and Na-carbonates collected from the PKFC showed variable ^{13}C compositions that indicate mixed carbon sources, including bedrock carbonate, atmospheric CO_2, and organic carbon (Wilson et al., 2011). Therefore, more accurate estimates of the net sequestration of CO_2 through passive carbonation will need to account for carbonate recycling, which can be particularly relevant in the case of kimberlite residues (Paulo et al., 2021). Given the stoichiometry of calcite dissolution (Eq. (4)), where 1 mol of calcite reacts with 1 mol of CO_2, the passive carbonation rate formula (R; Eq. (1)) can be corrected by subtracting the mole transfer predicted for the dissolution of calcite ($m CaCO_3$) from the mole transfer of CO_2 ($m CO_2$). This transformation generates a new rate

Table 5
Passive carbonation rates corrected (R^C) for carbonate dissolution in Diavik. Mineral trapping (M_T) as secondary carbonate minerals was determined using proportional molar equivalences of the secondary carbonate to CO_2. Solubility trapping (S_T) was calculated as R'-M_T.

Passive carbonation rates		Scenario 1: Lizardite		Scenario 2: Forsterite	
		g CO_2/m^2/yr	t CO_2/yr	g CO_2/m^2/yr	t CO_2/yr
Passive carbonation					
CO_2 consumption (total)	**$R(CO_2)$**	707	608	674	580
CO_2 in $CaCO_3$ dissolution	**$R(CaCO_3)$**	203	175	295	254
Passive carbonation (corrected)	**R^C**	**504**	**433**	**379**	**326**
Mineral trapping					
Nesquehonite		–	–	–	–
Trona		70	60	70	61
Nahcolite		105	90	86	74
Total Mineral trapping (total)	**M_T**	**175**	–	**156**	–
Solubility trapping	**S_T**	**329**	–	**222**	–

(R^c) described by Equation (5), where mCO_2 and $mCaCO_3$ correspond to the average CO_2 and calcite mole transfer per liter of solution, respectively. M_{CO2} is the molar mass of CO_2 (g/mol), A corresponds to the area (m^2) of the mine waste impoundments, and V is the volume of water (L/yr) used in mineral processing in 1 yr.

$$CaCO_3(s) + CO_2(g) + H_2O \rightarrow Ca^{2+} + 2HCO_3^- \quad (4)$$

$$R^c\left(g\,/\,m^2\,/\,yr\right) = [mCO_2 - mCaCO_3] \times M_{CO2} \times [1\,/\,A] \times V \quad (5)$$

The predicted average mole transfer for each CO_2 mineralization scenario is summarized in Supplementary Table A, and the passive carbonation rates are plotted with time in Fig. 6. The mole transfers of CO_2 fluctuate, indicating that passive carbonation rates at Diavik are also changing over time (Fig. 6). For example, peaks in CO_2 mole transfers were observed mainly by the end of 2004 and at the beginning of 2005, suggesting that seasonality and mine residues management practices are likely to impact the CO_2 sequestration rates in active mines. Moreover, passive carbonation *(R)* peaks often coincided with calcite dissolution peaks (Fig. 6). The average CO_2 consumption rates (R) were calculated at ~710 and ~675 g CO_2/m^2/yr for the lizardite and forsterite dissolution scenarios respectively. Correction of these values for calcite dissolution (R') results in an average passive carbonation rate of ~375–510 g CO_2/m^2/yr. At these rates, the annual CO_2 sequestered at Diavik was estimated at ~320−440 t CO_2 (0.86 km^2) per year, reflecting mineral and solubility trapping (Table 5).

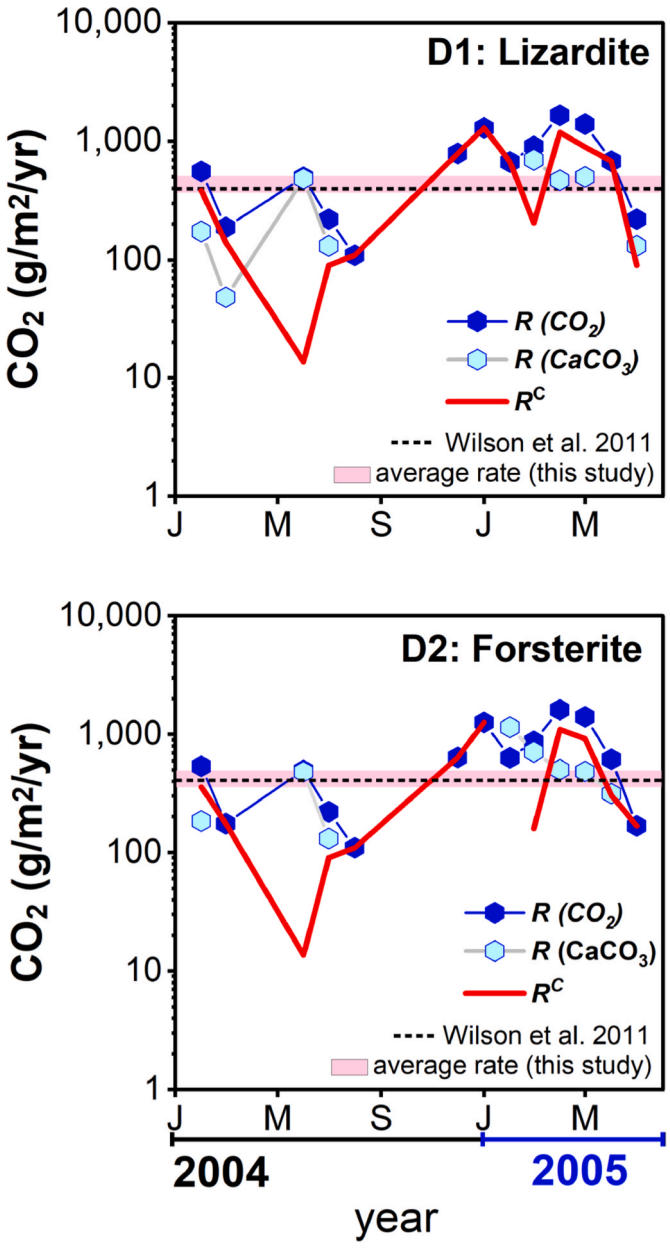

Fig. 6. Passive carbonation rates estimated from CO_2 ($R_{(CO2)}$) and calcite ($R_{(CaCO3)}$) mole transfer for the lizardite (D1) and forsterite (D2) inverse models for Diavik. The red line indicates the corrected passive carbonation (R'). The dashed line indicates the annual average passive carbonation estimated by Wilson et al. (2011) based on nesquehonite abundance in the tailings. The shaded pink area shows the average range for Diavik's passive carbonation calculated with inverse modeling.

The mass-balance models also predicted that trona and nahcolite precipitation at Diavik is linked to water chemistry variations. Wilson et al. (2011) reported that mineral trapping of CO_2 at Diavik occurs mainly as nesquehonite, but Na- and Ca-carbonate minerals are also present in crusts on the PKCF. These authors showed that based on the radiocarbon values ($0.9 \leq F^{14}C \leq 1$), approximately 89–100% of the carbon stored in secondary carbonate minerals is consistent with modern carbon sources (i.e., atmospheric and organic carbon). Mineralogical surveys have determined that ~1800 t CO_2 were trapped and stored within nesquehonite during the first six years of the mine's operations (Wilson et al., 2009). The corresponding average annual sequestration is 270–300 t of CO_2, given the percentage of modern carbon in the secondary carbonates (Wilson et al., 2011), which is equivalent to a passive carbonation rate of ~313–350 g CO_2/m^2/yr for the PKCF. If accounting for the carbon stored as trona and nahcolite determined by inverse modeling, mineral trapping would produce a rate of ~175–300 g CO_2/m^2/yr (Table 5). This rate is similar to the mineral trapping rate determined that Wilson et al. (2011) determined. Possible sources for Na in Diavik kimberlite residues include smectite and plagioclase (albite). In the absence of additional secondary carbonate minerals predicted by the model, we assumed that the remaining 200−210 g CO_2/m^2/yr are assigned to solubility trapping of CO_2 in waters. The possibility to predict and discriminate between mineral and aqueous sinks for CO_2 in active mines can be a noteworthy advantage of the geochemical modeling approach compared to mineralogical surveys.

4.3.3. *Venetia diamond mine*

Secondary Mg-carbonate minerals, which would provide unequivocal evidence for passive carbonation, have not been detected in Venetia mine residues. Instead, the mineralogical data from numerous samples collected from the FRD showed that calcite is the most abundant carbonate mineral in the mine residues (Mervine et al., 2018; Paulo et al., 2021; Stubbs et al., 2022; Zeyen et al., 2022). As predicted with PHREEQC, calcite is saturated (SI > 1) in the mine waters and is likely the main sink for CO_2 in the kimberlite residues (Fig. 5). However, the kimberlite ore also contains 4−10 wt% of primary calcite (Paulo et al., 2021; Zeyen et al., 2022), complicating the identification of secondary calcite in the processed kimberlite. Thus, mineral abundance does not work well as a proxy for passive carbonation rates in this case. Therefore, using mass-balance models can be advantageous because of their ability to predict carbonate dissolution and precipitation reactions.

Calcite precipitation was predicted in scenarios dominated either by the dissolution of diopside (scenario V1), tremolite (scenario V2), or lizardite (scenario V3) (Table 6). These minerals account for approximately 35 wt% of the kimberlite mineral assemblage (Table 2). On average, the mass-balance scenarios linked to diopside dissolution resulted in greater CO_2 mole transfer (1.1×10^{-2} mol/L), followed by the tremolite (6.9×10^{-3} mol/L), and lizardite (3.5×10^{-3} mol/L) scenarios (Table 6). A stoichiometric equivalence of 1:1 between calcite precipitated and the CO_2 consumed was frequently observed in monthly estimates of mole transfer rates (Table 6). Albite (plagioclase) dissolution is enhanced at high pH and salinity (Gruber et al., 2019), and albite is also predicted to dissolve in all models (9.0×10^{-3} mol/L). This mineral can be a source of Na in solution in addition to smectite. The

Table 6
Average mole transfers (mol/L) for the different minerals in scenario V1 (diopside), V2 (forsterite), and V3 (lizardite) using the flow path defined from the North Dam and FRD for the common data from 2004 to 2018. Positive values (+) correspond to phases dissolving (+), and negative values to mineral phases precipitating (−).

Venetia mine:	Scenario V1	Scenario V2	Scenario V3
Phases	(diopside)	(tremolite)	(lizardite)
Dissolution			
CO_2(g)	9.25×10^{-3}	5.42×10^{-3}	2.85×10^{-3}
Diopside	6.38×10^{-3}		
Magnetite	1.08×10^{-3}	1.08×10^{-3}	1.08×10^{-3}
Tremolite		1.28×10^{-3}	
Lizardite			2.12×10^{-3}
Albite	9.00×10^{-3}	9.00×10^{-3}	9.00×10^{-3}
Precipitation			
Calcite	-9.57×10^{-3}	-5.74×10^{-3}	-3.17×10^{-3}
SiO_2(am)	-1.28×10^{-2}	-1.02×10^{-2}	-4.24×10^{-3}
Smectite-low-Fe-Mg	-7.20×10^{-3}	-7.20×10^{-3}	-7.20×10^{-3}
Exchange			
NaX	-1.04×10^{-2}	-1.04×10^{-2}	-1.04×10^{-2}
CaX_2	3.43×10^{-3}	3.43×10^{-3}	3.43×10^{-3}
KX	3.50×10^{-3}	3.50×10^{-3}	3.50×10^{-3}

release of sodium into waters might enhance cation exchange in kimberlite, which promotes the replacement of calcium and magnesium from smectites and increases their availability for mineral trapping.

Calcite precipitation has been documented in several laboratory studies as a by-product of diopside (pyroxene) and tremolite (amphibole) dissolution (Diedrich et al., 2018; Kalinkina et al., 2001; Ryu et al., 2011; Stockmann et al., 2008, 2013). Diopside dissolution is typically incongruent at low temperatures (25−70 °C) and over a wide pH range (Knauss et al., 1993; Stockmann et al., 2008). The release of Ca from diopside is generally much greater than Mg and Si, (Knauss et al., 1993), and calcium carbonate coatings (calcite, aragonite) can form directly on dissolving diopside surfaces without inhibiting mineral dissolution (Stockmann et al., 2008, 2013). Tremolite also releases calcium preferentially, yet calcite has only been reported to form at high temperatures (290 °C) (Diedrich et al., 2018; Ryu et al., 2011). Thus, calcite precipitation due to tremolite dissolution is unlikely to occur under Venetia mine conditions.

Previous batch dissolution experiments using Venetia kimberlite residues (CO_2 >99%, 25 °C) suggested that lizardite is the dominant source of Mg in the kimberlites (Paulo et al., 2021). The reaction of serpentine minerals with CO_2 generates Mg-carbonates + quartz ± H_2O, yet only calcite was identified as the main carbon sink for CO_2 in scenario 3 (Table 6). It is possible that given the high pH of the waters, silicate dissolution is rather limited, and Mg concentrations in waters are insuficient to induce Mg-carbonate saturation. On the other hand, a direct correspondence between the mole transfer of calcite and Ca exchanged (CaX_2, where X corresponds to the exchange master species) was often observed in the inverse modeling results (Table 6). These results are consistent with cation exchange being an important source of cations for CO_2 mineralization in kimberlite mine residues in addition to mineral dissolution (Zeyen et al., 2022). Given the high smectite content of the kimberlite (up to 40 wt%), it is expected that interlayer cations will be exchanged with aqueous cations in mine waters (Odom, 1984). Calcium is the most abundant element that can be extracted via cation exchange (3.8−10.4 g Ca/kg versus 0.3−2.3 g Mg/kg) from Venetia kimberlites (Zeyen et al., 2022). The positive CaX_2 and negative NaX, along with the smectite mole transfer predicted by inverse modeling simulations, support the hypothesis that Ca is likely released and replaced by Na in the clays during wetting periods (e.g., $CaX_2 + 2Na^+ = Ca^{2+} + 2NaX$). Furthermore, the replacement of Ca^{2+}or Mg^{2+} by Na^+ in the exchange sites on clay surfaces can be fostered in waters with low Na (Zou et al., 2021), like those of Venetia. Therefore, it is likely that cation exchange also affects CO_2 mineralization in kimberlites.

Using the long-term water chemistry records (2009–2018) from Venetia mine enabled the detection of CO_2 sequestration patterns during the mine lifetime, illustrated by changes in the mass balance for CO_2, calcite, diopside, and CaX_2 (Fig. 7a). These trends show that calcite precipitation increases in periods with greater consumption of CO_2, diopside, and greater exchange of calcium (CaX_2). The changes in CO_2 mole transfer are reflected in the passive carbonation rates (Fig. 7b) and provide insights into the long-term efficacy of the impoundments in retaining CO_2. Because passive carbonation (R) rates from 2015 to 2018 account for the monthly water volume and mass of kimberlite processed, this period correlates more strongly with possible effects of mine residue storage practices and the water budget used in kimberlite slurries (Fig. 7). For example, a peak in passive carbonation rates (2000 g $CO_2/m^2/yr$, Fig. 7b−c) estimated for 2016 results from a significant increase in kimberlite processing and, consequently, water usage. The annual average passive carbonation rate, based on the CO_2 mole transfer in the diopside model, was estimated to vary from 300 to 770 g $CO_2/m^2/yr$ (Fig. 7a). These rates agree with estimates recently obtained for unweathered kimberlite (200−900 g $CO_2/m^2/yr$) based on direct CO_2 fluxes into Venetia kimberlite residues measured with CO_2 flux chambers (Stubbs et al., 2022). Moreover, the calcite precipitation mole transfer translates into a passive carbonation rate of 145–770 g $CO_2/m^2/yr$. The passive carbonation rate suggests that most CO_2 reacting with the kimberlite has been stored as a solid phase (calcite) within the mine wastes.

The total mass of CO_2 sequestered from 2009 to 2018 in Venetia kimberlite residues was calculated from the definite integral (Eq. (2)) defined by the passive carbonation function (Fig. 7b). The use of the definite integral function is advantageous because it allows for CO_2 sequestration rates to be monitored at different intervals, helping with verification of the impact of mine waste production in carbon capture. Using this technique for the nine years of operation, we estimated that the kimberlite residues stored ~4250 g CO_2/m^2 (Fig. 7b) primarily as calcite at an average passive carbonation rate of ~470 g $CO_2/m^2/yr$. Limiting the integral to the period between 2015 and 2018, for which calculations used the precise volume of the water in the kimberlite slurries, the passive carbonation of the kimberlite residues contributed to the sequestration of 1450 g CO_2/m^2 which is equivalent to an average passive carbonation rate of ~480 g $CO_2/m^2/yr$. Assuming the average 6.28×10^{-3} mol/L of calcite precipitation in the mine wastes (Table 6) and at a slurry deposition rate of 3×10^6 m^3/yr, the mass of calcite would increase by ~1700 t/yr in the FRD. Considering that the annual production of fine kimberlite residues is 2.8 Mt/yr, this would imply that the abundance of calcite in the mine wastes would increase by 0.07 wt% or 700 mg/kg. The quantification of passive carbonation rates with QXRD at Venetia is largely complicated by the heterogeneity of the feedstocks, the occurrence of abundant pre-existing calcite, and the relatively low mass changes in carbonate minerals. The carbonation rate of Venetia kimberlites is particularly complex to evaluate due to their variable calcite content, which ranges from 4 to 10 wt% (Zeyen et al., 2022). These small changes in calcite abundance would unlikely be detectable with QXRD. Thus, when dealing with such significant heterogeneity, minor changes in calcite abundance are unlikely to be detected through crystallographic assessments or even total inorganic carbon analysis, as recently reported by Stubbs et al. (2022). Our results suggest that using mass-balance models is perhaps a better assessment tool for quantifying mineral trapping in mineralogically complex mining wastes, particularly when CO_2 is being stored in calcite that also occurs as a gangue mineral.

A potential offset of 1.5% of Venetia's annual emissions (0.21 Mt/yr, Mervine et al. (2018)) was previously reported for the FRD based on the maximum uptake of CO_2 by residues dominated by the dark volcanoclastic kimberlite facies (Stubbs et al., 2022). Similarly, we estimated that an offset of ~1% is likely achieved today through passive carbonation at Venetia mine, which corresponds to ~1700 t CO_2 being stored

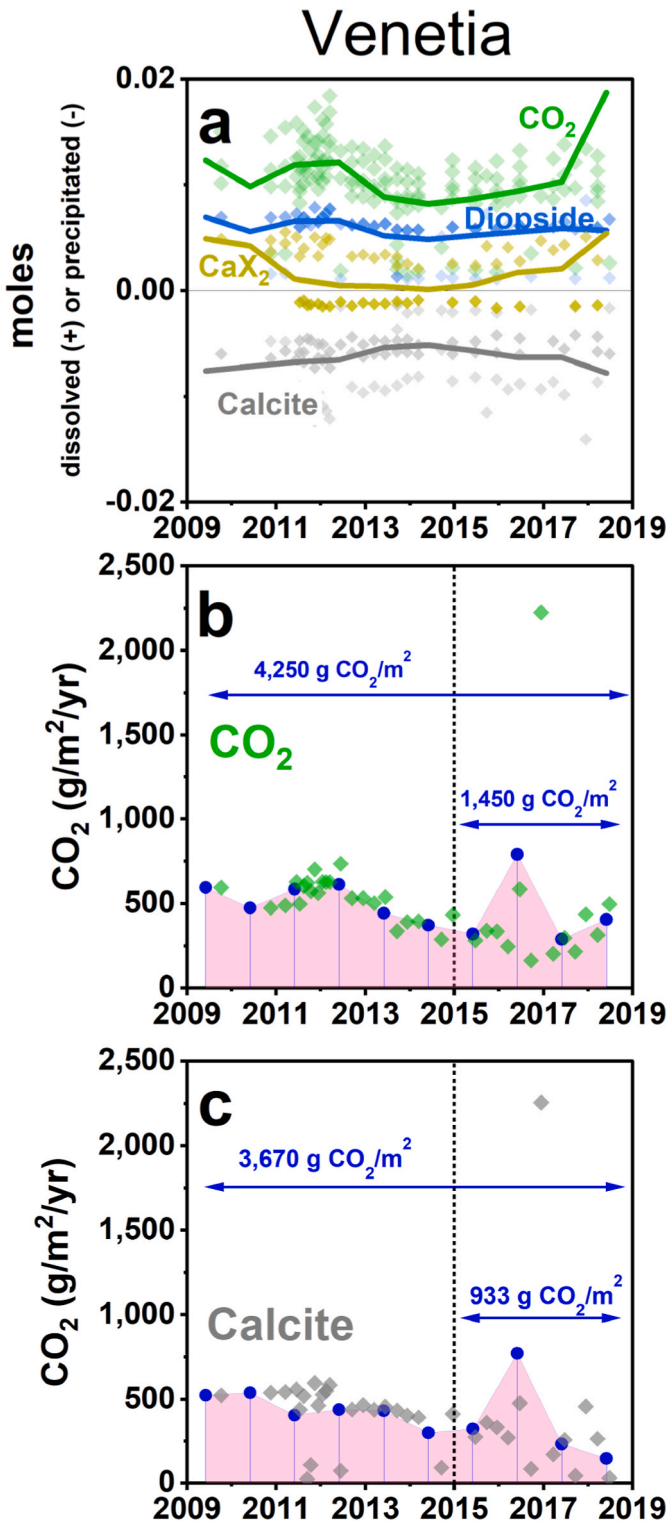

Fig. 7. (a) Mole transfer (diamond symbols) simulated for CO_2, diopside, CaX_2, and calcite. The lines represent the average mole transfer for each phase. (b) Distribution of the passive carbonation rates (g $CO_2/m^2/yr$) for Venetia FRD between 2009 and 2018 based on CO_2 mole transfer. (c) Distribution of the passive carbonation rates (g $CO_2/m^2/yr$) for Venetia FRD between 2009 and 2018 based on calcite mole transfer. Results after 2015 were influenced by changes in the availability of operational data (tonnes of kimberlite and water usage). Average annual passive carbonation (blue dots; calculated for equal 1 yr intervals) and the area highlighted (pink) were used to calculate the definite integral.

annually within mine residues with the current mine waste management practices. However, our model also shows a general decreasing trend in the passive carbonation rate (Fig. 7b), suggesting that carbon sequestration in the mine residues at Venetia may become less effective over time. Changes in the bulk geochemistry of the kimberlite residues, loss of reactivity, or excess water in the impoundments are important factors that limit CO_2 mineralization reactions (Stubbs et al., 2022). Therefore, efforts to increase or maintain carbon sequestration rates at Venetia will require adopting new management strategies. Some of these strategies may include introducing physical modifications to the mine residue impoundments, such as expanding the area available for processed kimberlite disposal, reducing the thickness of the mine waste layers, and minimizing flooding (Stubbs et al., 2022). Alternatively, utilizing kimberlite residues as a soil amendment for enhanced rock weathering can foster mineral weathering reactions and increase CO_2 consumption.

5. Implications for carbon accounting at the mine scale

Unintentional passive carbonation demonstrates the ability of tailings to sequester CO_2 and offers an opportunity for mines to introduce management practices that enhance this process. Ideally, mining operations would claim carbon offsets resulting from accelerating passive carbonation to contribute toward meeting carbon neutrality goals. However, frequent and extensive sampling of mine residues for mineralogical assessments may be limited due to analytical expenses, staffing, and potential safety risks at active mines. For example, submerged or saturated mine wastes (e.g., tailings) are not easily or safely accessed, limiting the ability to sample all parts of a mine residue storage compound as part of a monitoring program. For these reasons, there is a need to develop more simple carbon measurement, reporting, and validation methodologies for active mines. As demonstrated in this study, inverse geochemical modeling is a valuable alternative to extensive sampling and analysis needed to estimate passive carbonation rates based on mine waste mineralogy.

Passive carbonation rates based on mass-balance calculations were consistent with those previously determined using mineralogical assessments (Table 7). The main differences between the two methodologies are that inverse modeling requires much less sampling and relies on information regularly reported as part of the mine's environmental monitoring programs and mineral processing activities (e.g., bulk mineralogy and environmental and operational data). Moreover, given the time covered by environmental monitoring data, mass-balance models can help track carbon sequestration rates over time, as discussed for Venetia. The continuous monitoring of CO_2 sequestration with mass-balance models is highly advantageous as it could enable mine managers to report and recognize patterns between CO_2 sequestration, waste management practices, and seasonality. These correlations can support decisions to introduce new practices to enhance and optimize CO_2 removal.

Hamilton et al. (2021) discussed the technical limitations of only using QXRD analysis to assess passive carbonation within mine wastes. The authors highlighted the inability of XRD to detect relatively low abundances of amorphous carbonate phases and distinguish between pre-existing and newly formed calcite, which can significantly affect rate estimations, as shown here in the case of Venetia. Alternatively, combining QXRD and total inorganic carbon data can better estimate passive carbonation rates, as the latter method quantifies both crystalline and amorphous carbonate phases. However, this approach still likely requires the analysis of 10s–100s of samples and overlooks the amount of CO_2 sequestered as a soluble phase (i.e., solubility trapping), which can be a substantial sink for atmospheric carbon, as suggested by the Diavik model. Inverse geochemical modeling also provides insights into the dominant mineral–water interactions influencing CO_2 sequestration rates within mine wastes, such as carbonate recycling in the system, which mineralogical assessments alone cannot determine. In addition, small changes in carbonate abundance are unlikely to be

Table 7
Comparison of the passive carbonation rates for active ultramafic mines estimated with different methodologies.

Passive carbonation $g\ CO_2/m^2/yr$	Mount Keith		Diavik		Venetia		
	samples	R avg.	samples	R range	samples	R range	R avg.
Mineralogical assessments	172	2,400[1]	20	313–350[2]	–	–	–
CO_2 fluxes[3]	–	–	–	–	1	200–900[4]	–
Geochemical modeling[4]	2	3900	32	375–510	72	300–770	472

(–) no data; [1]Wilson et al., (2014); [2]Wilson et al., (2011); [3]Stubbs et al., (2022); [4] this study.

detected and quantified using methods mentioned prior when mineral heterogeneity is a predominant characteristic of the mine wastes, such as observed for the kimberlites. Thus, integrating geochemical modeling as a regular practice for carbon accounting in active mines can be more advantageous than mineralogical assessments.

Mine waste impoundments are closed basins in which the slurries deposition exerts the most control of the basin hydrology. Thus, the passive carbonation rates presented here combine the mass balance results with the volume of processing water, assuming this volume is the primary water input. As described, the passive carbonation rate was calculated using a constant water budget (Table 2), corresponding to the volume (flow) of the processing water used per tonne of ore into the mine residues impoundments. However, a better knowledge of a mine's water budget is desirable to improve further the model predictions. As shown for Venetia, using the exact mass-to-water ratio deposited in the impoundments between 2015 and 2018 produces a more comprehensive and dynamic analysis of the impact of the mine production on the passive carbonation rate. In addition, atmospheric precipitation (i.e., volume and chemical composition of rain and snow) could also be accounted for in models, since its accumulation in the impoundments is expected to increase the transfer of atmospheric CO_2 into tailings and contribute further to mineral reactions. Given that the fluid-to-mineral ratio in mine wastes strongly impacts mineral carbonation at ambient temperature (Stubbs et al., 2022), accounting for the total volume of water reacting with mine waste will help increase the accuracy of the model predictions. As such, detailed water budgets are recommended to improve the model's ability to track CO_2 more accurately and provide more rigorous long-term monitoring assessments for carbon sequestration in active mines.

On the other hand, improving the accuracy of mass-balance models for passive carbonation monitoring will largely depend on the quality and the frequency of collection of water chemistry data. Our inverse modeling calculations assume a steady-state and that water samples along a flow path were obtained on the same date (Parkhurst and Appelo, 2013). The mass balance also assumes that changes in water chemistry are related to mineral dissolution and precipitation, but it does not account for reaction kinetics, temperature, or the spatial variability of aqueous geochemistry (Parkhurst and Appelo, 2013). Because mass-balance models determine the differences between an initial and final water composition, missing information in the datasets can compromise the ability to predict the products of mineral carbonation accurately and also imply greater uncertainty limits (i.e., variation allowed for the concentration of each element in the solution to run a model). For example, an increase in Si concentrations in waters provides evidence for silicate mineral dissolution in the mine residues. However, Si concentrations were usually absent or sporadically analyzed and reported in the datasets. Furthermore, reporting alkalinity or dissolved inorganic carbon more frequently will also improve the quality of estimates for CO_2 sequestration. In some cases, alkalinity was also absent (e.g., Diavik) from datasets which necessitated the use of hardness as a substitute for carbonate alkalinity in waters. Finally, incorporating stable isotope data (e.g., $\delta^{18}O$ and $\delta^{2}H$) into the model could also improve our understanding of the extent to which water chemistry is affected by mixing with meteoric precipitation and evaporation (Chad et al., 2022). Thus, we recommend systematically measuring dissolved Si, alkalinity, and stable isotopes to help reduce model uncertainty and produce more accurate predictions of passive carbonation in active mines.

Finally, ultramafic mines can be considered enhanced rock weathering demonstration projects where rock powders are continuously dispersed over land with the advantage that environmental monitoring programs are already in place to support carbon accounting. Consequently, mine residue impoundments can play a crucial role in researching and developing acceleration technologies for ERW that reduce the dependency on large land footprints while simplifying MVR by containing CO_2 removal within closed basins. For instance, mines are ideal sites to test and develop new chemical, biological, and physical strategies (Hamilton et al., 2021; Stubbs et al., 2022; Zeyen et al., 2022) to accelerate the removal of atmospheric CO_2 via mineral weathering processes. Developing such strategies will provide a wider range of solutions for implementing ERW technologies.

5.1. Passive carbonation of ultramafic mine wastes on a global scale

Most ultramafic mines produce hundred of kilotonnes to tens of megatonnes per year of pulverized rock that has the capacity for CO_2 sequestration (Paulo et al., 2021; Power et al., 2020); however, their collective contribution to global CO_2 consumption is still poorly constrained. Interestingly, the passive carbonation rates estimated for the studied mines are comparable to or greater than those estimated for the world's largest rivers indicating that weathering is accelerated in mine wastes impoudments filled with rock powders (Fig. 8). The rates of CO_2 consumption linked to mineral weathering based on river water chemistry are estimated to vary from 1 to 338 g $CO_2/m^2/yr$, with greater rates observed in basins dominated by carbonate or basaltic bedrock (Gaillardet et al., 1999). We estimated that kimberlite mine residues with high surface areas have weathering rates comparable to those measured in the Kikori River basin, Papua New Guinea (338 g $CO_2/m^2/yr$), even though this basin is dominated by carbonate and basalt lithologies that are more reactive to CO_2.

While completely offsetting mine emissions with passive carbonation rates may be possible at certain types of mines (e.g., Mount Keith), most mines will only sequester a fraction of their GHG emissions via passive carbonation. For most mines, greater carbon removals through passive carbonation are mostly constrained by the area available for spreading mine wastes since the CO_2 removal rates in the mines are much greater than natural weathering rates. However, given the worldwide distribution of ultramafic mine, passive carbonation and enhanced weathering of mine wastes is expected to have a global impact on carbon removal efforts. More than 21,000 mine sites, including 129 diamond mines, have been delineated globally with an estimated area of 57,277 km^2, accordingly to the visual interpretation of satellite images of the land area corresponding to the active mines included in the SNL metals and mining database (S&P Global Market Intelligence) (Maus et al., 2020). If the surface areas of all diamond mine residue impoundments are similar to those of Diavik (0.86 km^2) and Venetia (3.5 km^2), the global land footprint of kimberlite residues likely corresponds to 110−450 km^2. As a result, passive carbonation of kimberlite residues alone may contribute to the sequestration of 0.04–0.21 Mt CO_2/yr, assuming rates for Diavik and Venetia are representative. There are 79 mines worldwide with more reactive mine residues, comprised mainly of olivine and serpentine minerals and possibly brucite (Bullock et al., 2021). If comparable in size to the Mount Keith nickel mine, tailings impoundments of these 79

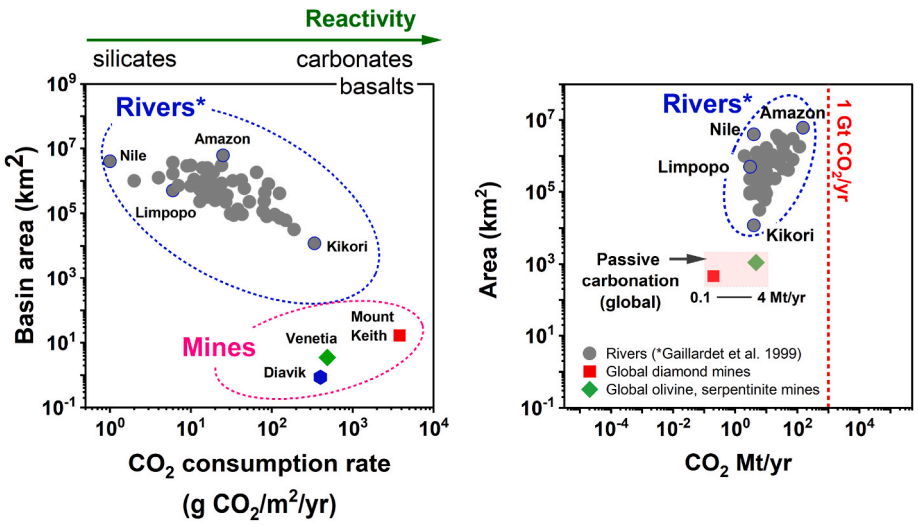

Fig. 8. (left) Comparison between the CO_2 consumption rates (g $CO_2/m^2/yr$) of the larger river basins in the world according to Gaillardet et al. (1999), and the passive carbonation rates estimated for Mount Keith, Diavik, and Venetia. (right) Estimates of global consumption of CO_2, in megatonnes (Mt/yr), associated with passive carbonation of diamond, olivine, and serpentinite mine residues compared to the annual consumption of CO_2 in rivers.

mines could occupy 1200 km^2. Assuming passive carbonation rates of ~3900 g/m^2/yr, these mines may be sequestering 4.3 Mt CO_2/yr (Fig. 8). These estimations assume that only the area of the mine residue impoundments is available for passive carbonation and illustrates the current baseline for passive carbonation at a global scale. Logically, scaling-up carbon removal via ERW requires expanding the area available to spread mineral powders, as recently demonstrated for very reactive magnesium oxide powders (Rausis et al., 2022). At the mine-scale level, the total land footprint of mines includes open pits, waste rock piles, and roads, which could be utilized for greater CO_2 sequestration. At Venetia, approximately 1700 t CO_2/yr are predicted to be currently sequestered in the 3.5 km^2 of the kimberlite residue impoundments. Increasing the rate of CO_2 removal via passive carbonation at Venetia could be achieved if residues are spread over an area of 10 km^2, dedicating 50% of the total footprint of the mine (~20 km^2) for carbon sequestration. This approach refers to the implementation of a low-cost technology where passive carbonation is accelerated exclusively by ERW, which implies the spreading of pulverized rock over large areas of land and assumes no changes to the mineral processing practices, or changes in mine waste disposal techniques. Venetia could sequester roughly three times more CO_2 per year (4900 t CO_2/yr) in the kimberlite residues, maintaining similar production rates. Thus, the introduction of accelerated weathering technologies in active mines, such as the redesign of the mine residues facilities, will be necessary to maximize the capacity of mines to remove CO_2 and achieve carbon neutrality targets faster.

6. Conclusions

Passive carbonation occurs spontaneously in ultramafic mine residues due to mineral–water reactions. Passive carbonation rates depend strongly on process water chemistry as well as climate since evaporation of mine waters is typically required to precipitate carbonate minerals. Moreover, passive carbonation rates in active mines are affected by the amount of ore processed and the volume of slurries deposited in mine waste impoundments. Changes in mine water chemistry reflect ongoing mineral dissolution and precipitation reactions, which can be used to determine baseline CO_2 consumption rates for active mines with geochemical modeling (inverse modeling). As demonstrated by this study, geochemical modeling produces estimates similar to those obtained from mineralogical and geochemical surveys that measure the amount of CO_2 stored by secondary carbonate minerals. Geochemical modeling only requires pre-existing information, such as mine water geochemistry and mine operational data, significantly reducing the need for an extensive or additional sampling of mine residues. Long-term monitoring of CO_2 sequestration can be done with geochemical modeling, enabling mine managers to report and recognize patterns between CO_2 sequestration, waste management practices, and seasonality. Further improvements to the inverse modeling approach as a predictive tool to estimate passive carbonation in active mines include.

- measuring and reporting dissolved Si, alkalinity, and stable isotopes in mine water chemistry data to reduce the model uncertainty related to silicate mineral dissolution, water evaporation, and mixing effects in water chemistry;
- using detailed water budgets for mines that account the exact volumes of water added to the mine waste impoundments.

In conclusion, our study demonstrates that geochemical modeling can be an alternative to more intensive methods used to measure carbon sequestration in active mines. Maximizing carbon sequestration in mine wastes is desirable since CO_2 mineralization and enhanced rock weathering have the potential to accelerate atmospheric carbon dioxide removal at the gigatonne scale (Beerling et al., 2020; Campbell et al., 2022). With the methodology presented here, we provide a more straightforward and manageable approach for measuring, validating, and reporting carbon removal by ultramafic mine tailings that is readily integrated into existing water quality monitoring.

Declaration of competing interest

The authors declare that they have no known competing financial interests or personal relationships that could have appeared to influence the work reported in this paper.

Data availability

The data that has been used is confidential.

Acknowledgments

We are grateful for the data and support while sampling at the Venetia Diamond Mine which was provided by De Beers Group of Companies. Evelyn Mervine, Jurgen De Swardt, and Chantelle DuPlessis

from the De Beers Group of Companies are thanked for assistance with data from the Venetia diamond mine. We also thank Alison Shaw from Lorax Environmental Service Ltd. For insightful comments. Funding was also provided by Natural Sciences and Engineering Research Council of Canada Discovery grants and a Natural Resources Canada Clean Growth grant to Power and Wilson, and a Mitacs Accelerate grant to Paulo, Power, Zeyen and Wilson. We also thank the insightful comments provided by the Associate Editor and reviewer that significantly improved this manuscript.

Appendix A. Supplementary data

Supplementary data to this article can be found online at https://doi.org/10.1016/j.apgeochem.2023.105630.

References

Amann, T., Hartmann, J., Struyf, E., de Oliveira Garcia, W., Fischer, E.K., Janssens, I., Meire, P., Schoelynck, J., 2020. Enhanced Weathering and related element fluxes – a cropland mesocosm approach. Biogeosciences 17, 103–119.

Aquatico Scientific, 2016. Annual Water Quality Assessment Report (2016) - Internal Report. DE BEERS Consolidated mines, Venetia Mine, p. 449.

Arvidson, R.S., Mackenzie, F.T., 1999. The dolomite problem; control of precipitation kinetics by temperature and saturation state. Am. J. Sci. 299, 257.

Assima, G.P., Larachi, F., Beaudoin, G., Molson, J., 2013a. Dynamics of carbon dioxide uptake in chrysotile mining residues – effect of mineralogy and liquid saturation. Int. J. Greenh. Gas Control 12, 124–135.

Assima, G.P., Larachi, F., Molson, J., Beaudoin, G., 2013b. Accurate and direct quantification of native brucite in serpentine ores—new methodology and implications for CO_2 sequestration by mining residues. Thermochim. Acta 566, 281–291.

Assima, G.P., Larachi, F., Molson, J., Beaudoin, G., 2014. Comparative study of five Québec ultramafic mining residues for use in direct ambient carbon dioxide mineral sequestration. Chem. Eng. J. 245, 56–64.

Ball, J.W., Nordstrom, D.K., 1991. WATEQ4F – User's manual with revised thermodynamic data base and test cases for calculating speciation of major, trace and redox elements in natural waters. Open File Rep. ed., p. 193. Series 91-183.

Bea, S.A., Wilson, S.A., Mayer, K.U., Dipple, G.M., Power, I.M., Gamazo, P., 2012. Reactive transport modeling of natural carbon sequestration in ultramafic mine tailings. Vadose Zone J. 11 vzj2011.0053.

Beaudoin, G., Nowamooz, A., Assima, G.P., Lechat, K., Gras, A., Entezari, A., Kandji, E.H. B., Awoh, A.-S., Horswill, M., Turcotte, S., Larachi, F., Dupuis, C., Molson, J., Lemieux, J.-M., Maldague, X., Plante, B., Bussière, B., Constantin, M., Duchesne, J., Therrien, R., Fortier, R., 2017. Passive mineral carbonation of Mg-rich mine wastes by atmospheric CO_2. Energy Proc. 114, 6083–6086.

Beerling, D.J., Kantzas, E.P., Lomas, M.R., Wade, P., Eufrasio, R.M., Renforth, P., Sarkar, B., Andrews, M.G., James, R.H., Pearce, C.R., Mercure, J.-F., Pollitt, H., Holden, P.B., Edwards, N.R., Khanna, M., Koh, L., Quegan, S., Pidgeon, N.F., Janssens, I.A., Hansen, J., Banwart, S.A., 2020. Potential for large-scale CO_2 removal via enhanced rock weathering with croplands. Nature 583, 242–248.

Bodénan, F., Bourgeois, F., Petiot, C., Augé, T., Bonfils, B., Julcour-Lebigue, C., Guyot, F., Boukary, A., Tremosa, J., Lassin, A., Gaucher, E.C., Chiquet, P., 2014. Ex situ mineral carbonation for CO_2 mitigation: evaluation of mining waste resources, aqueous carbonation processability and life cycle assessment (Carmex project). Miner. Eng. 59, 52–63.

Brand, N.W., Butt, C.R.M., 2001. Weathering, element distribution and geochemical dispersion at Mt Keith, Western Australia: implication for nickel sulphide exploration. Geochem. Explor. Environ. Anal. 1, 391–407.

Bricker, O.P., Jones, B.F., Bowser, C.J., 2003. 5.04 - mass-balance approach to interpreting weathering reactions in watershed systems. In: Holland, H.D., Turekian, K.K. (Eds.), Treatise on Geochemistry. Pergamon, Oxford, pp. 119–132.

Bullock, L.A., James, R.H., Matter, J., Renforth, P., Teagle, D.A.H., 2021. Global carbon dioxide removal potential of waste materials from metal and diamond mining. Frontiers in Climate 3.

Campbell, J.S., Foteinis, S., Furey, V., Hawrot, O., Pike, D., Aeschlimann, S., Maesano, C. N., Reginato, P.L., Goodwin, D.R., Looger, L.L., Boyden, E.S., Renforth, P., 2022. Geochemical negative emissions technologies: Part I. Review. Frontiers in Climate 4.

Chad, S.J., Barbour, S.L., McDonnell, J.J., Gibson, J.J., 2022. Using stable isotopes to track hydrological processes at an oil sands mine, Alberta, Canada. J. Hydrol.: Reg. Stud. 40, 101032.

Consulting, M.W.E.S., 2017. Mt Keith Satellite Pits Environmental Impact Assessment Hydrology Processes and Inland Water BHP Nickel West, p. 87.

Daval, D., Martinez, I., Corvisier, J., Findling, N., Goffé, B., Guyot, F., 2009. Carbonation of Ca-bearing silicates, the case of wollastonite: experimental investigations and kinetic modeling. Chem. Geol. 265, 63–78.

Deton' Cho Stantec, 2015. Lac de Gras Water Chemistry, Spatial Variability, and Temporal Trends, Final Report. Prepared for: Government of Northwest Territories, Yellowknife, NT X1A 2L9.

Diavik Diamond Mines Inc, 2020. North Inlet Water Treatment Plant Operations Plan Diavik Diamond Mines. Inc., p. 13, 2012.

Diedrich, T., Schott, J., Oelkers, E.H., 2018. An experimental study of tremolite dissolution rates as a function of pH and temperature: implications for tremolite toxicity and its use in carbon storage. Mineral. Mag. 78, 1449–1464.

Frondini, F., Vaselli, O., Vetuschi Zuccolini, M., 2019. Consumption of atmospheric carbon dioxide through weathering of ultramafic rocks in the voltri massif (Italy): quantification of the process and global implications. Geosciences 9, 258.

Gaillardet, J., Dupré, B., Louvat, P., Allègre, C.J., 1999. Global silicate weathering and CO_2 consumption rates deduced from the chemistry of large rivers. Chem. Geol. 159, 3–30.

Gautier, Q., Bénézeth, P., Mavromatis, V., Schott, J., 2014. Hydromagnesite solubility product and growth kinetics in aqueous solution from 25 to 75°C. Geochem. Cosmochim. Acta 138, 1–20.

Golder Associates Ltd., 2018. Processed Kimberlite Containment Facility. Diavik Diamond Mines, p. 73 (2012) Inc.

Graham, I., Burgess, J.L., Bryan, D., Ravenscroft, P.J., Thomas, E., Doyle, B.J., Hopkins, R., Armstrong, K.A., 1998. The Diavik kimberlites - lac de Gras, Northwest Territories, Canada. International Kimberlite Conference: Extended Abstracts 7, 259–261.

Gruber, C., Harlavan, Y., Pousty, D., Winkler, D., Ganor, J., 2019. Enhanced chemical weathering of albite under seawater conditions and its potential effect on the Sr ocean budget. Geochem. Cosmochim. Acta 261, 20–34.

Hamilton, J.L., Wilson, S.A., Turvey, C.C., Morgan, B., Tait, A.W., McCutcheon, J., Fallon, S.J., Southam, G., 2021. Carbon accounting of mined landscapes, and deployment of a geochemical treatment system for enhanced weathering at Woodsreef Chrysotile Mine, NSW, Australia. J. Geochem. Explor. 220, 106655.

Harrison, A.L., Power, I.M., Dipple, G.M., 2013. Accelerated carbonation of brucite in mine tailings for carbon sequestration. Environ. Sci. Technol. 47, 126–134.

Harrison, A.L., Dipple, G.M., Power, I.M., Mayer, K.U., 2015. Influence of surface passivation and water content on mineral reactions in unsaturated porous media: implications for brucite carbonation and CO_2 sequestration. Geochem. Cosmochim. Acta 148, 477–495.

Harrison, A.L., Mavromatis, V., Oelkers, E.H., Bénézeth, P., 2019. Solubility of the hydrated Mg-carbonates nesquehonite and dypingite from 5 to 35 °C: implications for CO_2 storage and the relative stability of Mg-carbonates. Chem. Geol. 504, 123–135.

Hartmann, J., Jansen, N., Dürr, H.H., Kempe, S., Köhler, P., 2009. Global CO_2-consumption by chemical weathering: what is the contribution of highly active weathering regions? Global Planet. Change 69, 185–194.

Haszeldine, R.S., Flude, S., Johnson, G., Scott, V., 2018. Negative emissions technologies and carbon capture and storage to achieve the Paris Agreement commitments. Phil. Trans. Math. Phys. Eng. Sci. 376, 20160447.

Huijgen, W.J.J., Witkamp, G.-J., Comans, R.N.J., 2006. Mechanisms of aqueous wollastonite carbonation as a possible CO_2 sequestration process. Chem. Eng. Sci. 61, 4242–4251.

IPCC, 2019. Climate Change and Land: an IPCC special report on climate change, desertification, land degradation, sustainable land management, food security, and greenhouse gas fluxes in terrestrial ecosystems. In: Shukla, P.R., Skea, J., Calvo Buendia, E., Masson-Delmotte, V., Pörtner, H.-O., Roberts, D.C., Zhai, P., Slade, R., Connors, S., van Diemen, R., Ferrat, M., Haughey, E., Luz, S., Neogi, S., Pathak, M., Petzold, J., Portugal Pereira, J., Vyas, P., Huntley, E., Kissick, K., Belkacemi, M., Malley, J. (Eds.), Climate Change and Land: an IPCC Special Report on Climate Change, Desertification, Land Degradation, Sustainable Land Management, Food Security, and Greenhouse Gas Fluxes in Terrestrial Ecosystems (in press).Technical Summary.

Kalinkina, E.V., Kalinkin, A.M., Forsling, W., Makarov, V.N., 2001. Sorption of atmospheric carbon dioxide and structural changes of Ca and Mg silicate minerals during grinding: II. Enstatite, åkermanite and wollastonite. Int. J. Miner. Process. 61, 289–299.

Knauss, K.G., Nguyen, S.N., Weed, H.C., 1993. Diopside dissolution kinetics as a function of pH, CO_2, temperature, and time. Geochem. Cosmochim. Acta 57, 285–294.

Lechat, K., Lemieux, J.-M., Molson, J., Beaudoin, G., Hébert, R., 2016. Field evidence of CO_2 sequestration by mineral carbonation in ultramafic milling wastes, Thetford Mines, Canada. Int. J. Greenh. Gas Control 47, 110–121.

Lu, P., Zhang, G., Apps, J., Zhu, C., 2022a. Comparison of thermodynamic data files for PHREEQC. Earth Sci. Rev. 225, 103888.

Lu, X., Carroll, K.J., Turvey, C.C., Dipple, G.M., 2022b. Rate and capacity of cation release from ultramafic mine tailings for carbon capture and storage. Appl. Geochem. 140, 105285.

Maus, V., Giljum, S., Gutschlhofer, J., da Silva, D.M., Probst, M., Gass, S.L.B., Luckeneder, S., Lieber, M., McCallum, I., 2020. A global-scale data set of mining areas. Sci. Data 7, 289.

Mervine, E.M., Wilson, S.A., Power, I.M., Dipple, G.M., Turvey, C.C., Hamilton, J.L., Vanderzee, S., Raudsepp, M., Southam, C., Matter, J.M., Kelemen, P.B., Stiefenhofer, J., Miya, Z., Southam, G., 2018. Potential for offsetting diamond mine carbon emissions through mineral carbonation of processed kimberlite: an assessment of De Beers mine sites in South Africa and Canada. Mineral. Petrol. 112, 755–765.

Meyer, N.A., Vögeli, J.U., Becker, M., Broadhurst, J.L., Reid, D.L., Franzidis, J.P., 2014. Mineral carbonation of PGM mine tailings for CO_2 storage in South Africa: a case study. Miner. Eng. 59, 45–51.

Minx, J.C., Lamb, W.F., Callaghan, M.W., Fuss, S., Hilaire, J., Creutzig, F., Amann, T., Beringer, T., de Oliveira Garcia, W., Hartmann, J., Khanna, T., Lenzi, D., Luderer, G., Nemet, G.F., Rogelj, J., Smith, P., Vicente Vicente, J.L., Wilcox, J., del Mar Zamora Dominguez, M., 2018. Negative emissions—Part 1: Research landscape and synthesis. Environ. Res. Lett. 13, 063001.

Moncur, M.C., Smith, L.J.D., 2012. Processed kimberlite porewater geochemistry from Diavik diamonds mines, Inc. In: PRICE, W.A. (Ed.), Proceedings from the 9th International Conference Acid Rock Drainage. Canada, 2012.
Moosdorf, N., Renforth, P., Hartmann, J., 2014. Carbon dioxide efficiency of terrestrial enhanced weathering. Environ. Sci. Technol. 48, 4809–4816.
Moss, S.W., Kobussen, A., Powell, W., Pollock, K., 2018. Kimberlite emplacement and mantle sampling through time at A154N kimberlite volcano, Diavik Diamond Mine: lessons from the deep. Mineral. Petrol. 112, 397–410.
Murray, J., Nordstrom, D.K., Dold, B., Kirschbaum, A., 2021. Seasonal fluctuations and geochemical modeling of acid mine drainage in the semi-arid Puna region: the Pan de Azúcar Pb–Ag–Zn mine, Argentina. J. S. Am. Earth Sci. 109, 103197.
National Academies of Sciences, E., and Medicine, 2019. Negative Emissions Technologies and Reliable Sequestration: A Research Agenda.
Neuner, M., Smith, L., Blowes, D.W., Sego, D.C., Smith, L.J.D., Fretz, N., Gupton, M., 2013. The Diavik waste rock project: water flow through mine waste rock in a permafrost terrain. Appl. Geochem. 36, 222–233.
Odom, I.E., 1984. Smectite clay minerals: properties and uses. Phil. Trans. Roy. Soc. Lond. Math. Phys. Sci. 311, 391–409.
Oskierski, H.C., Turvey, C.C., Wilson, S.A., Dlugogorski, B.Z., Altarawneh, M., Mavromatis, V., 2021. Mineralisation of atmospheric CO_2 in hydromagnesite in ultramafic mine tailings – insights from Mg isotopes. Geochem. Cosmochim. Acta 309, 191–208.
Parkhurst, D.L., 1997. Geochemical mole-balance modeling with uncertain data. Water Resour. Res. 33, 1957–1970.
Parkhurst, D.L., Appelo, C.A.J., 2013. Description of input and examples for PHREEQC version 3—a computer program for speciation, batch-reaction, one-dimensional transport, and inverse geochemical calculations. U.S. Geological Survey Techniques and Methods, p. 497 book 6, chap. A43. https://pubs.usgs.gov/tm/06/a43/.
Paulo, C., Power, I.M., Stubbs, A.R., Wang, B., Zeyen, N., Wilson, S.A., 2021. Evaluating Feedstocks for Carbon Dioxide Removal by Enhanced Rock Weathering and CO_2 Mineralization. Applied Geochemistry, 104955.
Power, I.M., Wilson, S.A., Thom, J.M., Dipple, G.M., Gabites, J.E., Southam, G., 2009. The hydromagnesite playas of Atlin, British Columbia, Canada: a biogeochemical model for CO_2 sequestration. Chem. Geol. 260, 286–300.
Power, I.M., Harrison, A.L., Dipple, G.M., Wilson, S.A., Kelemen, P.B., Hitch, M., Southam, G., 2013. Carbon mineralization: from natural analogues to engineered systems. Rev. Mineral. Geochem. 77, 305–360.
Power, I.M., McCutcheon, J., Harrison, A.L., Wilson, S.A., Dipple, G.M., Kelly, S., Southam, C., Southam, G., 2014. Strategizing carbon-neutral mines: a case for pilot projects. Minerals 4, 399–436.
Power, I.M., Harrison, A.L., Dipple, G.M., Wilson, S.A., Barker, S.L.L., Fallon, S.J., 2019. Magnesite formation in playa environments near Atlin, British Columbia, Canada. Geochem. Cosmochim. Acta 255, 1–24.
Power, I.M., Dipple, G.M., Bradshaw, P.M.D., Harrison, A.L., 2020. Prospects for CO_2 mineralization and enhanced weathering of ultramafic mine tailings from the Baptiste nickel deposit in British Columbia, Canada. Int. J. Greenh. Gas Control 94, 102895.
Rausis, K., Stubbs, A.R., Power, I.M., Paulo, C., 2022. Rates of atmospheric CO_2 capture using magnesium oxide powder. Int. J. Greenh. Gas Control 119, 103701.
Rollo, H.A., Jamieson, H.E., 2006. Interaction of diamond mine waste and surface water in the Canadian Arctic. Appl. Geochem. 21, 1522–1538.
Ryu, K.W., Lee, M.G., Jang, Y.N., 2011. Mechanism of tremolite carbonation. Appl. Geochem. 26, 1215–1221.
Sandalow, D., Aines, R., Friedmann, J., Kelemen, P., McCormick, C., Power, I.M., Schmidt, Brianna, Wilson, S.A., 2021. Carbon Mineralization Roadmap. ICEF Innovation Roadmap Project. November 2021.
Schuiling, R.D., Krijgsman, P., 2006. Enhanced weathering: an effective and cheap tool to sequester CO_2. Climatic Change 74, 349–354.
Smith, L.J.D., Moncur, M.C., Neuner, M., Gupton, M., Blowes, D.W., Smith, L., Sego, D.C., 2013. The Diavik Waste Rock Project: design, construction, and instrumentation of field-scale experimental waste-rock piles. Appl. Geochem. 36, 187–199.
Stockmann, G., Wolff-Boenisch, D., Gíslason, S.R., Oelkers, E.H., 2008. Dissolution of diopside and basaltic glass: the effect of carbonate coating. Mineral. Mag. 72, 135–139.
Stockmann, G.J., Wolff-Boenisch, D., Gislason, S.R., Oelkers, E.H., 2013. Do carbonate precipitates affect dissolution kinetics?: 2: diopside. Chem. Geol. 337–338, 56–66.
Stripp, G.R., Field, M., Schumacher, J.C., Sparks, R.S.J., Cressey, G., 2006. Post-emplacement serpentinization and related hydrothermal metamorphism in a kimberlite from Venetia, South Africa. J. Metamorph. Geol. 24, 515–534.
Stubbs, A.R., Paulo, C., Power, I.M., Wang, B., Zeyen, N., Wilson, S.A., 2022. Direct measurement of CO_2 drawdown in mine wastes and rock powders: implications for enhanced rock weathering. Int. J. Greenh. Gas Control 113, 103554.
Sun, W., Jayaraman, S., Chen, W., Persson, K.A., Ceder, G., 2015. Nucleation of metastable aragonite CaCO3 in seawater. Proc. Natl. Acad. Sci. U. S. A. 112, 3199–3204.
Taylor, L.L., Driscoll, C.T., Groffman, P.M., Rau, G.H., Blum, J.D., Beerling, D.J., 2021. Increased carbon capture by a silicate-treated forested watershed affected by acid deposition. Biogeosciences 18, 169–188.
Thom, J.G.M., Dipple, G.M., Power, I.M., Harrison, A.L., 2013. Chrysotile dissolution rates: implications for carbon sequestration. Appl. Geochem. 35, 244–254.
Turvey, C.C., Wilson, S.A., Hamilton, J.L., Southam, G., 2017. Field-based accounting of CO_2 sequestration in ultramafic mine wastes using portable X-ray diffraction. Am. Mineral. 102, 1302–1310.
Turvey, C.C., Wilson, S.A., Hamilton, J.L., Tait, A.W., McCutcheon, J., Beinlich, A., Fallon, S.J., Dipple, G.M., Southam, G., 2018. Hydrotalcites and hydrated Mg-carbonates as carbon sinks in serpentinite mineral wastes from the Woodsreef chrysotile mine, New South Wales, Australia: controls on carbonate mineralogy and efficiency of CO_2 air capture in mine tailings. Int. J. Greenh. Gas Control 79, 38–60.
Voigt, M., Marieni, C., Clark, D.E., Gíslason, S.R., Oelkers, E.H., 2018. Evaluation and refinement of thermodynamic databases for mineral carbonation. Energy Proc. 146, 81–91.
Wilson, S.A., Raudsepp, M., Dipple, G.M., 2009. Quantifying carbon fixation in trace minerals from processed kimberlite: a comparative study of quantitative methods using X-ray powder diffraction data with applications to the Diavik Diamond Mine, Northwest Territories, Canada. Appl. Geochem. 24, 2312–2331.
Wilson, S.A., Dipple, G.M., Power, I.M., Barker, S.L., Fallon, S.J., Southam, G., 2011. Subarctic weathering of mineral wastes provides a sink for atmospheric CO_2. Environ. Sci. Technol. 45, 7727–7736.
Wilson, S.A., Harrison, A.L., Dipple, G.M., Power, I.M., Barker, S.L.L., Ulrich Mayer, K., Fallon, S.J., Raudsepp, M., Southam, G., 2014. Offsetting of CO_2 emissions by air capture in mine tailings at the Mount Keith Nickel Mine, Western Australia: rates, controls and prospects for carbon neutral mining. Int. J. Greenh. Gas Control 25, 121–140.
Zeyen, N., Wang, B., Wilson, S.A., Paulo, C., Stubbs, A.R., Power, I.M., Steele-Maclnnis, M., Lanzirotti, A., Newville, M., Paterson, D.J., Hamilton, J.L., Jones, T.R., Turvey, C.C., Dipple, G.M., Southam, G., 2022. Cation exchange in smectites as a new approach to mineral carbonation. Frontiers in Climate 4.
Zhang, S., Bai, X., Zhao, C., Tan, Q., Luo, G., Wang, J., Li, Q., Wu, L., Chen, F., Li, C., Deng, Y., Yang, Y., Xi, H., 2021. Global CO_2 consumption by silicate rock chemical weathering: its past and future. Earth's Future 9, e2020EF001938.
Zou, Y., Zheng, C., Sheikhi, S., 2021. Role of ion exchange in the brine-rock interaction systems: a detailed geochemical modeling study. Chem. Geol. 559, 119992.